



Published in final edited form as:

Cell Rep. 2021 March 16; 34(11): 108858. doi:10.1016/j.celrep.2021.108858.

Organization and emergence of a mixed GABA-glycine retinal circuit that provides inhibition to mouse ON-sustained alpha retinal ganglion cells

Abhilash Sawant^{1,2}, Briana N. Ebbinghaus^{1,3}, Adam Bleckert⁴, Clare Gamlin⁴, Wan-Qing Yu⁴, David Berson⁵, Uwe Rudolph^{6,7}, Raunak Sinha^{1,2,3}, Mrinalini Hoon^{1,2,3,8,*}

¹Department of Ophthalmology and Visual Sciences, University of Wisconsin-Madison, Madison, WI, USA

²Department of Neuroscience, University of Wisconsin-Madison, Madison, WI, USA

³McPherson Eye Research Institute, University of Wisconsin-Madison, Madison, WI, USA

⁴Department of Biological Structure, University of Washington, Seattle, WA, USA

⁵Department of Neuroscience, Brown University, Providence, RI, USA

⁶Department of Comparative Biosciences, College of Veterinary Medicine, University of Illinois at Urbana-Champaign, Champaign, IL, USA

⁷Carl R. Woese Institute for Genomic Biology, University of Illinois at Urbana-Champaign, Champaign, IL, USA

⁸Lead contact

SUMMARY

In the retina, amacrine interneurons inhibit retinal ganglion cell (RGC) dendrites to shape retinal output. Amacrine cells typically use either GABA or glycine to exert synaptic inhibition. Here, we combined transgenic tools with immunohistochemistry, electrophysiology, and 3D electron microscopy to determine the composition and organization of inhibitory synapses across the dendritic arbor of a well-characterized RGC type in the mouse retina: the ON-sustained alpha RGC. We find mixed GABA-glycine receptor synapses across this RGC type, unveiling the existence of “mixed” inhibitory synapses in the retinal circuit. Presynaptic amacrine boutons with dual release sites are apposed to ON-sustained alpha RGC postsynapses. We further reveal the sequence of postsynaptic assembly for these mixed synapses: GABA receptors precede glycine receptors, and a lack of early GABA receptor expression impedes the recruitment of glycine

This is an open access article under the CC BY-NC-ND license (<http://creativecommons.org/licenses/by-nc-nd/4.0/>).

*Correspondence: mhoon@wisc.edu.

AUTHOR CONTRIBUTIONS

M.H. and R.S. designed research. A.S., B.N.E., A.B., C.G., W.-Q.Y., D.B., R.S., and M.H. performed research. A.S., B.N.E., A.B., C.G., W.-Q.Y., D.B., and M.H. analyzed data. U.R. contributed new reagents. A.S., R.S., and M.H. wrote the paper.

SUPPLEMENTAL INFORMATION

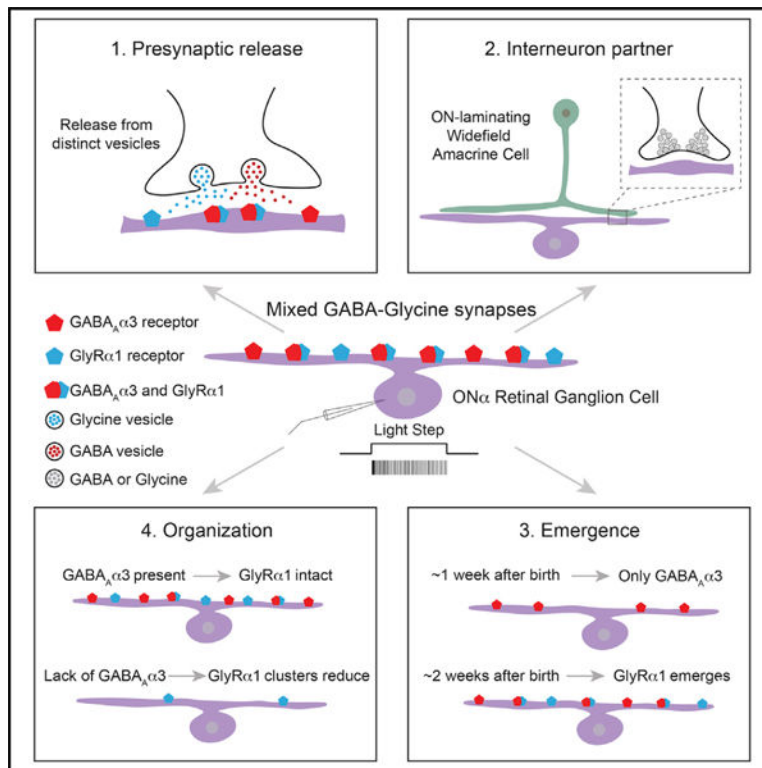
Supplemental Information can be found online at <https://doi.org/10.1016/j.celrep.2021.108858>.

DECLARATION OF INTERESTS

The authors declare no competing interests.

receptors. Together our findings uncover the organization and developmental profile of an additional motif of inhibition in the mammalian retina.

Graphical abstract



In brief

Sawant et al. show the occurrence of mixed GABA-glycine synapses across the dendrites of a well-characterized retinal output neuron, where GABA and glycine are released from distinct presynaptic vesicles putatively by a widefield interneuron. Emergence of receptors at these synapses is temporally offset during development with GABA receptors recruiting glycine receptors.

INTRODUCTION

A common feature of neural circuits is the tight interplay between excitation and inhibition that sculpts both spontaneous and evoked activity (Isaacson and Scanziani, 2011). In sensory systems such as the retina and olfactory sensory neurons, circuit inhibition can lead to feature selectivity such as direction selectivity (Wei and Feller, 2011), orientation selectivity (Antinucci and Hindges, 2018), and approach sensitivity (Münch et al., 2009) and can also regulate the behavioral response of an organism (e.g., odor-evoked inhibition of sensory neurons can itself evoke attraction-avoidance behaviors; Cao et al., 2017). The composition and organization of inhibitory motifs have thus been a topic of active investigation across circuits. A common circuit principle is the rich diversity of interneurons that can provide

synapse-specific inhibition across specific compartments of a principal neuron (e.g., basket versus chandelier interneuronal input across pyramidal neuron; Thomson and Jovanovic, 2010) or contribute to specific neural computations (e.g., in the retinal circuit, where AII and A17 interneurons specifically process dim-light signals; Hoon et al., 2014; Wässle, 2004). Interneuronal diversity is most appreciated in the inner mammalian retina (Helmstaedter et al., 2013; MacNeil and Masland, 1998), where the functional characteristics, connectivity, and organizational principles (pre- and postsynaptic specializations) remain unknown for the vast majority of amacrine cell (AC) interneurons. ACs shape the output responses of retinal ganglion cells (RGCs), which ferry visual information from the retina to higher brain centers (Hoon et al., 2014; Masland, 1988; Nirenberg and Meister 1997; Wässle, 2004). ACs mediate postsynaptic inhibition on the soma and/or dendrites of RGCs either via the neurotransmitter GABA or glycine, and in general GABA-releasing ACs extend dendritic arbors over a wider spatial extent than glycinergic ACs (Koulen et al., 1996; Wässle et al., 1998; Zhang and McCall, 2012). Added to the diversity of ACs is the diversity of RGC types (Baden et al., 2016; Sanes and Masland, 2015; Völgyi et al., 2009), with only a few RGC types well characterized in terms of their roles in visual processing and their retinal synaptic connectivity.

In this study, we focused on inhibitory postsynapses across a well-characterized murine RGC type called the ON-sustained alpha RGC (henceforth referred to as “ON α ”). The ON α exhibits a sustained depolarizing response to light increments across luminosities (Krieger et al., 2017) and is the RGC type most sensitive to dim-light signals, carrying single-photon visual information to higher brain areas (Smeds et al., 2019). The excitatory circuit for the ON α has been delineated, and it is known which bipolar cell type (type 6) provides the majority of excitatory input and how these excitatory inputs regulate ON α visual responses (Schwartz et al., 2012). Previous work has shown that GABA_A receptors and glycine receptor alpha-1 subunit-containing (GlyR α 1) synapses mediate postsynaptic inhibition on ON α (Koulen et al., 1996; Majumdar et al., 2007). However, the molecular composition and developmental profile of inhibitory synapses providing postsynaptic inhibition across ON α RGCs remain undetermined. We combined murine transgenic tools with single-cell electrophysiology and serial electron microscopy (EM) to determine the molecular composition of inhibitory synapses across ON α s and the synaptic mechanism of GABA and glycine release from ACs onto ON α s and uncovered the identity of an “ON” laminating AC type that provides inhibitory input to ON α . We further probed the development of inhibitory synapses across ON α and uncovered a key role of early GABA_A receptors for establishment of ON α inhibitory synapses. Together our findings have revealed an additional motif of retinal inhibition on a well-characterized RGC type that revises our understanding of how specific inhibitory circuits are organized to regulate visual processing in the mammalian retina.

RESULTS

GABA and glycine receptors colocalize on ON α RGC dendrites

The ON α receives both dim and bright light information via rod and cone photoreceptors, respectively (Figure 1A). Rod and cone photoreceptor signals reach the ON α through well-

characterized parallel pathways that ultimately converge at cone bipolar cell terminals, which make glutamatergic synapses onto ON α dendrites (Figure 1A; see also Hoon et al., 2014; Wässle, 2004). To determine the composition of inhibitory, GABA, and glycinergic synapses across the ON α dendritic arbor that mediate postsynaptic inhibition onto this cell, we used a specific mouse transgenic line (*Thy1-YFPH*) in which a subset of RGCs are fluorescently labeled. The ON α is one of the RGC types labeled in this line (Bleckert et al., 2013, 2014) and can be unambiguously identified by its characteristic morphology and dendritic lamination pattern (Bleckert et al., 2013, 2014; Krieger et al., 2017). Adult *Thy1-YFPH* retinas were co-labeled with antibodies against GABA $_A$ and GlyR α 1 receptor subunits, as previous studies have shown that mouse ON α s get input from both GABA and glycinergic ACs through GABA $_A$ and GlyR α 1 receptors, respectively (Koulen et al., 1996; Majumdar et al., 2007; Wässle et al., 1998). To determine which GABA $_A$ receptor type is expressed across ON α arbors, we co-labeled retinas with antibodies against GlyR α 1 and either α 3 subunit-containing GABA $_A$ receptors (GABA $_A\alpha$ 3; Figure 1) or α 1 subunit-containing GABA $_A$ receptors (GABA $_A\alpha$ 1; Figure S1). These two GABA $_A$ receptor types were selected because they are most likely to provide inhibition on ON α arbors, as GABA $_A\alpha$ 1-, GABA $_A\alpha$ 2-, and GABA $_A\alpha$ 3-containing GABA $_A$ receptors are the main GABA $_A$ receptor types present at distinct non-overlapping synapses in the inner retinal synaptic layer (Wässle et al., 1998) and because GABA $_A\alpha$ 2 receptors are specifically localized to a non-ON α RGC inhibitory circuit (Greferath et al., 1995). Very few GABA $_A\alpha$ 1 receptor puncta were found to be distributed across ON α dendrites (Figure S1A), confirming that this receptor type is not a prominent component of GABAergic inhibition across ON α s. In corroboration, when we quantified expression of GABA $_A\alpha$ 1 across ON α dendrites, we observed negligible percentage occupancy of GABA $_A\alpha$ 1 across ON α arbors (volume of receptor pixels relative to volume of ON α arbor; Figure S1B). In contrast, GABA $_A\alpha$ 3 puncta were abundantly localized across the ON α arbor, where they were closely associated with GlyR α 1 puncta (Figure 1B). The observation of colocalized GABA $_A\alpha$ 3 and GlyR α 1 receptor clusters within the ON α dendritic arbor was striking, as previous studies of GABA and glycine receptor distribution in the inner synaptic layer of the mouse and rat retina have reported a non-overlapping distribution pattern of these receptor subtypes (mouse retina, Frazao et al., 2007; rat retina, Sassoè-Pognetto et al., 1995). We next quantified the percentage colocalization between the GlyR α 1 puncta within the ON α RGCs and the GABA $_A\alpha$ 3 receptor signal (see STAR Methods for details) and determined ~55% of true colocalization between these receptor types (true colocalization = total colocalization – random colocalization after 90° flip of GABA $_A\alpha$ 3 channel; Figure 1C; Figure S1C). Thus, our analyses revealed that ~55% of ON α RGC GlyR α 1 receptor-containing postsynapses also have GABA $_A\alpha$ 3 receptors. Together our observations revealed the GABA $_A$ receptor type that is expressed across ON α s and also uncovered a population of “mixed” GlyR α 1-GABA $_A\alpha$ 3 postsynapses across the mouse ON α .

Mechanism of GABA-glycine neurotransmitter release onto ON α RGC dendrites

Given our observation of mixed GlyR α 1-GABA $_A\alpha$ 3 postsynapses across the ON α , the next question we addressed was, what is the presynaptic mechanism of GABA and glycine release onto the ON α ? Figure 2A illustrates four possible scenarios by which GABA and glycine release from AC boutons could activate mixed GlyR α 1-GABA $_A\alpha$ 3 receptors: (I)

presynaptic terminals with synaptic vesicles containing (and co-releasing) both GABA and glycine, (II) presynaptic terminals with a mixed pool of distinct synaptic vesicles containing either GABA or glycine, (III) presynaptic terminals apposed to mixed GlyR α 1-GABA α 3 receptors with dedicated pools of synaptic vesicles filled with either GABA or glycine, and (IV) two different presynaptic AC terminals releasing GABA and glycine at close proximity. To differentiate between these possibilities, we performed whole-cell patch-clamp recordings from ON α RGCs (Figure 2B) and analyzed the amplitude and frequency of miniature inhibitory postsynaptic currents (mIPSCs) in the presence of glutamate receptor blockers (NBQX and D-AP5) and tetrodotoxin (TTX) to block the voltage-gated sodium channels. We reasoned that if GABA and glycine were co-released from the same presynaptic vesicle (Figure 2A, scenario I), upon application of the GABA α receptor blocker GABAzine (exemplar mIPSC trace with and without GABAzine in Figure 2C), we would see a decrease in overall amplitude of ON α mIPSCs and no change in the frequency of ON α mIPSC events. In contrast, if GABA and glycine were released through distinct presynaptic vesicles (Figure 2A, scenarios II–IV), we would see a decrease in the frequency of ON α mIPSCs and no change in the amplitude of ON α mIPSC events after GABAzine application. Upon quantifying ON α mIPSC amplitude (Figure 2D) and frequency (Figure 2E) of events before versus after GABAzine application, we observed a significant reduction in mIPSC event frequency but not amplitude after GABAzine application (Figures 2D and 2E). We next repeated the same mIPSC experiment in the presence of the glycine receptor blocker strychnine (Figure S2) and again observed a significant reduction in mIPSC frequency but no change in mIPSC amplitude after strychnine application (Figures S2B and S2C).

Inhibitory input on ON α RGCs can be mediated by both spiking and non-spiking ACs (Park et al., 2018). Thus, to account for all spontaneous inhibitory synaptic release on ON α RGCs, we performed recordings from ON α s without TTX (but in the presence of glutamate receptor blockers) and analyzed the amplitude and frequency of these spontaneous inhibitory postsynaptic currents (sIPSCs) before and after application of GABAzine (Figure S3). Consistent with the mIPSC recordings, we observed a significant reduction in sIPSC event frequency after application of GABAzine without any change in sIPSC amplitude (Figures S3D and S3E). Of note, previous sIPSC recordings pooled across all mouse alpha RGC types mention no noticeable effect of GABAzine application (Majumdar et al., 2007). However, our recordings specifically from ON α RGCs show a robust effect of GABAzine on sIPSC event frequency (Figure S3E; average \pm SEM: control, 17.81 ± 0.16 ; +GABAzine, 9.46 ± 1.02 ; $p = 0.000297$). We also analyzed the distribution of both the rise time and decay time of ON α RGC mIPSC (Figures S2D and S2E) and sIPSC (Figures S3F and S3G) events and observed a unimodal (see also STAR Methods) distribution in the control condition (before GABAzine) and after GABAzine application (Figures S2 and S3). This precluded us from separating mIPSC and sIPSC events into GABAergic or glycinergic events on the basis of their kinetics. Taken together, our results from both the mIPSC and sIPSC experiments suggest that GABA and glycine are not co-released from the same presynaptic vesicle onto the ON α arbor.

GABA-glycine co-transmission could be mediated by ON-laminating widefield ACs

Our recordings from ON α RGCs preclude co-release of GABA and Glycine from the same presynaptic vesicle and point to three possible presynaptic arrangements for ON α mixed GABA and glycine synapses (scenarios II–IV). To identify which is the prevalent scenario and gain insight into the ultrastructural arrangement of AC synaptic boutons across the ON α , we performed serial block face scanning EM (SBFSEM) and reconstructed the ultrastructural arrangements of inhibitory synapses across the ON α RGC. The *Thy1-YFPH* line was used to locate an ON α , and near infrared branding (NIRBing; see Bishop et al., 2011; Bleckert et al., 2013; Della Santina et al., 2016) was used to create fiduciary marks surrounding the ON α to enable localization and reconstruction at the EM (Figure 3A). The ON α RGC soma and proximal dendritic arbors were reconstructed and all sites of inhibitory input identified and annotated (Figure 3B; see STAR Methods for criteria of synapse annotation). We observed two distinct arrangements of presynaptic AC boutons apposed to sites of inhibitory input across the ON α arbor. One class contained a single synaptic vesicle pool clustered across the synaptic sites, whereas the second class contained two or more clusters of synaptic vesicles at distinct sites apposed to a single postsynaptic thickening (site) akin to our expectations from scenario III (Figures 3C–3C’). We thereafter classified inhibitory synapses as “single” (one pool of synaptic vesicles), “dual” (two distinct synaptic vesicle pools/release sites, verified across two or three consecutive EM planes), triple (with three pools of synaptic vesicles), or, rarely observed, quadruple (with four pools), and we quantified the number of these inhibitory synapse types across the proximal ON α RGC arbor (Figure 3D). We observed that ~60% of inhibitory synapses across the ON α have a single release pool, and about ~40% of inhibitory synapses across the ON α have a presynaptic bouton with multiple distinct synaptic vesicle release sites (Figure 3D). The presence of a single presynaptic bouton containing multiple release sites apposed to an ON α synapse would favor scenario III (i.e., a single AC releasing GABA and glycine from distinct release sites). To determine whether this arrangement of inhibitory synapses was restricted to the proximal dendritic arbor of the ON α as observed in our NIRBing SBFSEM dataset (Figures 3A–3D) or whether a similar distribution could be observed across a wider region of the ON α dendritic arbor, we used the k0725 SBFSEM dataset (Briggman lab; Ding et al., 2016) to trace and fully reconstruct all of the ON α dendritic arbor (see STAR Methods for details) included within the volume of this EM stack. We mapped all the inhibitory synapses across the ON α arbor within the k0725 dataset (Figure 3E) and quantified its distribution. Once again, we classified inhibitory synapses as “single” or “dual” on the basis of the number of synaptic vesicle pools apposed to a postsynaptic site. We observed dual synapses distributed across both proximal and distal segments of the ON α dendritic arbor (Figure 3E) and a similar proportion of inhibitory synapses with single (~60%; Figure 3F) and multiple (~40%; Figure 3F) release sites, consistent with our quantifications of the synapse distribution along the proximal ON α RGC dendritic arbor (Figure 3D). Of note in our determination of the ultrastructural arrangements of AC boutons apposed to ON α arbors both in the NIRBed and in the k0725 dataset, we did not observe any postsynaptic site with two closely arranged presynaptic boutons (i.e., scenario IV arrangements). Together our observations revealed the ultrastructural arrangement of AC terminals apposed to inhibitory synapses across the ON α and uncovered that about 40% of

inhibitory input onto the ON α arrives through AC boutons with multiple synaptic vesicle release sites.

To uncover the morphological identity of ACs that provide input onto the ON α at dual release sites, which could be suggestive of GABA and glycine release at distinct sites, we reconstructed profiles of ACs providing inhibitory input to the ON α using the k0725 dataset. In this dataset, we could reconstruct three ACs and trace the neurites that provide input to ON α at dual synaptic vesicle release sites all the way back to the soma at the inner nuclear layer (Figure 4). All three ACs thus identified were widefield ACs that laminated in the “ON” plexus coincident with the arborization of the ON α . We thus refer to this AC type as ON-laminating widefield ACs (ON-WACs). Of note, all three examples of reconstructed ON-WACs showed no dendritic processes at other laminae of the inner plexiform layer. All three ON-WACs provided the majority of inhibitory input onto the ON α arbor at boutons with dual synaptic vesicle release sites (Figures 4A–4C). Given the extent of the dataset, we could reconstruct only one portion of the dendritic arbor for the second ON-WAC (Figures 4B–4B’). On average, all three reconstructed ON-WACs provided ~40 inhibitory synapses with dual synaptic vesicle release sites onto the ON α arbor. Upon analyses of the ON-WAC->ON α RGC synaptic bouton diameter, we observed that ON-WAC presynaptic boutons with dual release sites were significantly larger than those with a single release site (Figure S4A). We next determined the identity of all ON-WAC output (inhibitory) synapses to RGCs (both ON α and other/non-ON α RGC types), bipolar cells and other ACs (Figures S4B–S4D). We found that of the total ON-WAC->RGC output synapses, the majority were to the ON α RGC (~69%; Figure S4B). The ON α RGC also received the majority of the ON-WAC->RGC synapses with dual synaptic vesicle release sites (~60%; Figure S4B). When considering the ON-WAC output synapses across all inner retinal cell types (RGCs, other ACs, and bipolar cells), the ON α RGC received the majority of the ON-WAC output synapses with dual synaptic vesicle release sites (~54%), and other ACs received the majority of the ON-WAC output synapses with a single synaptic vesicle release site (~77%; Figures S4C and S4D). Thus, ON α RGCs are the main RGC postsynaptic partner for ON-WACs and ON-WACs preferentially synapse onto ON α RGCs with multiple release sites. Taken together, our observations uncovered the identity of an inhibitory input onto the ON α that occurs through ON-WACs via presynaptic boutons with primarily dual synaptic vesicle release sites.

GABA_A receptors localize prior to glycine receptors across ON α RGC dendrites

To determine the timeline of ON α inhibitory synapse organization, we next immunolabeled for GABA_A α 3 and GlyR α 1 synapses and determined the expression of these receptor subtypes across ON α dendrites at four developmental time points (Figure 5): postnatal day 8 (P8), P12, P16, and P21. As eye opening in rodents is around P14, our selection includes two time points before and two time points after eye opening. Our experiments were performed in the *Thy1-YFPH* mouse line to enable visualization of ON α RGCs and to isolate receptor signal specifically within the ON α (Figure 5). At P8, only GABA_A α 3 receptor signal was observed within the ON α dendritic arbor, and negligible GlyR α 1 signal could be detected across ON α cells at this time point (Figure 5A). From P12 till P21, both GABA_A α 3 and GlyR α 1 were robustly expressed within ON α RGCs (Figure 5A). We also immunolabeled for the inhibitory postsynaptic scaffolding protein gephyrin within

developing ON α s (Figure 5B). Gephyrin is known to scaffold all glycine receptors and a subset of retinal GABA $_A$ receptors primarily those containing GABA $_A\alpha$ 2 or GABA $_A\alpha$ 3 receptor subunits (Sassoè-Pognetto et al., 1995; Sassoè-Pognetto and Wässle, 1997). We found robust gephyrin expression within ON α arbors as early as P8 and maintenance of this expression profile all through circuit formation (till P21; Figure 5B). Next we quantified the expression level of each synaptic marker (GABA $_A\alpha$ 3, GlyR α 1, and gephyrin) within P8, P12, P16, and P21 ON α dendrites by determining the volume occupancy of each marker normalized to the RGC dendritic volume (percentage occupancy; Figure 5C). At P8, both GABA $_A\alpha$ 3 and gephyrin are present at comparable amounts within ON α dendrites, with no detectable GlyR α 1 expression (Figure 5C). By P12, GlyR α 1 expression within ON α dendrites reaches its mature levels, and GABA $_A\alpha$ 3 levels at P12 also significantly increase compared with P8 levels (Figure 5C). Gephyrin maintains its expression levels within ON α RGCs across time points, and the ON α GABA $_A\alpha$ 3/GlyR α 1 expression ratio remains relatively constant from P12 to P21. Taken together, our observations show that the scaffolding protein gephyrin is present within ON α s at mature amounts as early as 1 week after birth and that GABA $_A$ receptor expression precedes GlyR expression across the ON α RGC.

Early GABA $_A\alpha$ 3 receptor expression is necessary for recruiting GlyR α 1 and organizing inhibitory synaptic sites across the ON α RGC

Our observation of early GABA $_A\alpha$ 3 expression within ON α RGCs (Figure 5) indicates that GABA $_A\alpha$ 3 might play a role for the developmental organization of mixed GABA $_A$ -GlyR synapses across the ON α arbor. To test this possibility and the dependence of ON α GlyR α 1 expression on the presence of early GABA $_A\alpha$ 3, we used a GABA $_A\alpha$ 3-knockout (α 3KO) mouse (Yee et al., 2005) and determined the expression of GlyR α 1 receptors across α 3KO ON α RGCs (Figure 6). To visualize ON α RGCs in the α 3KO, we crossed the α 3KO line into the *Thy1-YFPH* transgenic background. GlyR α 1 synaptic puncta were drastically downregulated across α 3KO ON α RGCs (Figure 6A), with significantly less total GlyR receptor puncta, dendritic GlyR puncta, and somatic GlyR puncta in α 3KO ON α s compared with control (Figure 6B). Of note, the total number of GlyR puncta remaining within α 3KO ON α s was ~45% of the control level (Figure 6B: littermate control total GlyR α 1 puncta within ON α = 1,564.25 \pm 254.67, α 3KO total GlyR α 1 puncta within ON α = 709 \pm 88.1). As ~55% of GlyR α 1 puncta within ON α s are colocalized with GABA $_A\alpha$ 3 (Figure 1C), this would mean that the fraction of ON α GlyR α 1 that is lost in the α 3KO represents the fraction associated with GABA $_A\alpha$ 3 at mixed synaptic sites. To determine if the loss of GlyR α 1 receptors in the α 3KO was specific to the mixed synapses across the ON α arbor, we next determined the GlyR α 1 expression on two other alpha RGC types, OFF sustained and OFF transient, that are known to receive robust glycinergic input (Murphy and Rieke, 2006) and that express GlyR α 1 receptors across their dendritic arbors (Zhang et al., 2014). We observed comparable GlyR α 1 distribution across the dendritic arbors of both OFF-sustained and OFF-transient RGCs in α 3KO retinas compared with control (Figure S5). Of note, the GlyR α 1 synaptic sites across the OFF RGCs do not appear colocalized with GABA $_A\alpha$ 3 receptor clusters (Figure S6), providing further evidence that only mixed GABA $_A\alpha$ 3-GlyR α 1 synaptic clusters are impaired in the α 3KO. Taken together our

observations underscore a selective disruption of GABA_Aα3-GlyRα1 mixed synapses across the α3KO ONα RGCs.

We further compared the distribution of excitatory postsynapses across α3KO and littermate control ONα RGCs by biolistic expression of the glutamatergic postsynaptic scaffolding protein PSD-95, known to recognize sites of glutamatergic input across the arbors of these RGCs (Schwartz et al., 2012). We observed comparable distribution of PSD-95 puncta across α3KO and control ONα RGC arbors (Figure S7A), verifying that excitatory input onto α3KO RGC remains unperturbed.

To determine the presence of remaining GABA_A receptor subunits across α3KO ONα RGCs, we next determined the expression of GABA_Aγ2 receptor subunits across α3KO ONαs compared with control. We used the *Thy1-YFPγ2* transgenic line to visualize GABA_Aγ2 receptor expression across RGCs (Bleckert et al., 2013) and crossed this line into the α3KO background. GABA_Aα3 receptors are known to co-assemble with GABA_Aγ2 subunits in the retina (Greferath et al., 1995) and GABA_Aα3 receptor puncta on ONα RGC dendrites colocalize with GABA_Aγ2 and gephyrin puncta (Figure 7A). In the α3KO, GABA_Aγ2 receptor expression within ONα RGCs is dramatically reduced compared with control (Figures 7B and 7D), confirming the absence of any functional GABA_A receptors across the dendritic arbors of α3KO ONαs. In further support, the other GABA_A receptor type normally present at minimal amounts across ONα RGC arbors (GABA_Aα1; Figure S1) is not upregulated across α3KO ONα RGCs (Figures S7B and S7C). Finally, we assessed the levels of gephyrin across α3KO ONαs by labeling for gephyrin and quantifying the amount of gephyrin in α3KO and control ONα RGCs (Figures 7C and 7D). The number of gephyrin puncta across α3KO ONα RGCs was comparable with control amounts, unveiling that the mechanisms controlling gephyrin recruitment to ONα RGC synapses are not regulated by GABA_Aα3. Together our observations in the α3KO revealed that the molecular organization of inhibitory synapses across the ONα RGCs is disrupted in the absence of early GABA_Aα3 expression, such that both GABA_A and glycine receptors are not accrued and clustered correctly at inhibitory synaptic sites across GABA_Aα3 deficient ONα RGCs, but the scaffolding protein gephyrin remains at these sites independent of the absence of clustered inhibitory receptors.

DISCUSSION

Inhibition in the retina is mediated by GABAergic and glycinergic ACs, ~50% of retinal inhibition is mediated by GABAergic ACs, and ~50% is mediated by glycinergic ACs (Hoon et al., 2014; Wässle, 2004; Wässle et al., 2009). Morphological studies have categorized these two AC subsets as occupying distinct non-overlapping synaptic sites in the retinal synaptic layer (Koulen et al., 1996), unlike inhibitory synapse organization in the brainstem and spinal cord, where postsynaptic sites with colocalized GABA and glycine receptors are often observed (Frazao et al., 2007; Todd et al., 1996) and presynaptic interneurons co-release both inhibitory neurotransmitters (Jonas et al., 1998). Here we identified an inhibitory circuit onto a well-characterized mammalian RGC that is composed of mixed GABA-glycine receptor synapses (i.e., the same postsynapse containing both GABA_Aα3 and GlyRα1 receptors). Combining electrophysiology and SBFSEM, our data reveal that the

inhibitory neurotransmitters GABA and glycine are not co-released from the same synaptic vesicle but rather released via distinct synaptic vesicles at release sites within a single presynaptic AC bouton. Tracing the processes of AC types that provide inhibitory input at dual release sites onto the ON α arbor, we uncovered three examples of ON-WACs with similar morphology. Tracking the developmental profile of inhibitory synapses across ON α dendrites revealed that the GABA α 3 receptor localizes at ON α synapses prior to the emergence of GlyR α 1 receptors. The early GABA α 3 receptor accumulation is critical for recruitment of GlyR α 1 at ON α “mixed” synapses, as GlyR α 1 receptor sites are significantly downregulated across the ON α arbor in the α 3KO retina compared with control. The GABA γ 2 subunit is also downregulated across α 3KO ON α arbors compared with control, confirming the lack of aggregated GABA α receptors without the early organizational role of GABA α 3. Together our findings reveal the existence of a mixed GABA-glycinergic circuit in the mammalian retina, trace the profile of a putative GABA-glycine co-releasing AC type, and determine the molecular assembly and organizational inter-dependence of this synapse type.

A selective “mixed” GABA-glycine inhibitory circuit in the mammalian retina

The enormous diversity among retinal ACs has precluded a complete anatomical and functional characterization of ACs. But previous studies on the organization of retinal inhibitory synapses have often reported distinct localization of GABAergic and glycinergic postsynaptic sites (Frazao et al., 2007; Koulen et al., 1996; Wässle et al., 1998) and a non-overlapping expression pattern of GABA and glycinergic presynaptic markers (Haverkamp and Wässle, 2000). Only a recent high-throughput single-cell RNA sequencing study showed the presence of an AC population that was positive for both GABA synthetic enzymes and the transporter expressed by glycinergic ACs (Yan et al., 2020). Our findings are in keeping with this observation, as the mixed GABA α 3-GlyR α 1 inhibitory circuit we find is a subset (~55% of all ON α GlyR synapses) of all the retinal inhibitory synapses. Our findings also shed light on the receptor composition of inhibitory synapses distributed across the ON α . We find three distinct populations of inhibitory synapses that mediate postsynaptic inhibition on the ON α RGC: mixed GABA α 3-GlyR α 1 synapses, GlyR α 1-only synapses, and GABA α 3-only synapses. Previous studies have shown the expression of GlyR α 1 receptors on ON α RGCs (Majumdar et al., 2007; Wässle et al., 1998), presence of GlyR-mediated inhibitory postsynaptic currents in ON α RGCs (Majumdar et al., 2007), and their potential contribution toward spike output (Murphy and Rieke, 2006). The A8 glycinergic amacrine of the mouse retina has been shown to provide inhibitory input to ON α RGCs through GlyR α 1-containing synapses (Lee et al., 2015), and a GABAergic CRH (corticotropin-releasing hormone)-expressing AC has been shown to provide inhibitory input onto the ON α primarily for the duration of positive contrast stimulus (Park et al., 2018). Thus, on the basis of our observations and previous studies, one can presume that the CRH GABAergic ACs provide inhibitory input to ON α s at GABA α 3-containing synapses. ON α RGCs exhibit a sustained action potential firing response to light increments (Krieger et al., 2017; Murphy and Rieke, 2006) over a wide dynamic range of visual input spanning both dim- and bright-light stimuli (Grimes et al., 2014). In addition to a robust excitatory glutamatergic drive from ON bipolar cells (Schwartz et al., 2012), ON α RGCs have been shown to receive inhibitory input during both positive and negative contrast stimuli (i.e.,

during light onset and offset) (Park et al., 2018; van Wyk et al., 2009), and this inhibitory input is mediated by both GABA_A and glycine receptors (Majumdar et al., 2007; Murphy and Rieke, 2006; Park et al., 2018). Our data reveal the identity of an ON-WAC that could provide inhibitory input to ONαs at dual release sites with putative mixed GABA-GlyRs. Future studies elaborating the light-evoked responses of the ON-WAC are needed to determine its functional properties, although its lamination profile would suggest that it has a depolarizing response to light onset (“ON” response), and it could thus provide inhibitory input to ONαs during positive contrast stimuli.

Our findings of colocalized GABA_Aα3 and GlyRα1 receptor sites across the ONα represent mixed GABA-glycine postsynapses in the retinal circuit. Colocalization of GABA and glycine receptors is, however, not uncommon among spinal cord and brainstem circuits (Frazao et al., 2007; Gamlin et al., 2018; Todd et al., 1996). In the avian auditory brainstem, mixed GABA-GlyR synapses have faster response kinetics than inhibitory synapses containing only GABARs (Kuo et al., 2009), and GABA can speed up GlyR-mediated synaptic currents (Lu et al., 2008), thereby refining the temporal window of inhibition at these synapses. Thus, co-transmission of GABA and glycine could be a means for enhancing the temporal resolution of inhibition in the mature auditory system (Lu et al., 2008). Mixed GABA and GlyR synaptic sites can also serve roles during development of brainstem circuits. For example, in developing abducens motor neurons, co-release of GABA and glycine increases reliability and optimizes inhibition of motor neuron function (Russier et al., 2002). But a purely developmental role of mixed GABA_A-GlyR synapses on the ONα is unlikely given the continued presence of this mixed circuit in the mature retina. Additional studies that assess the functional properties of ONα RGCs upon selective disruption of GABAR synapses, GlyR synapses, and mixed GABAR-GlyR synapses are needed to determine the contribution of each of these inhibitory motifs on regulating the output of ONαs. As ONα RGCs are critical components of the dim-light visual circuit ferrying single-photon signals to higher visual centers (Smeds et al., 2019), unveiling how postsynaptic inhibition and the underlying circuit components modulate ONα signaling is crucial to understand the retinal substrates for dim light vision.

GABA_Aα3 as an early developmental recruiter of GlyRα1 to retinal mixed synapses

Across the CNS, GABA_Aα3 receptors are often expressed during early periods of development (Bosman et al., 2002; Laurie et al., 1992; Liu and Wong-Riley, 2004). In the adult, GABA_Aα3 receptors occupy a rather restricted distribution representing 10%–20% of expressed GABA_A receptors (Fritschy and Mohler, 1995; McKernan and Whiting, 1996; Pirker et al., 2000). In monoaminergic neurons of the CNS, GABA_Aα3 receptors are the main GABA_A receptor subtype (Fritschy and Mohler, 1995). Consequently, the α3KO mouse shows behavioral signatures of functional hyperactivity in the midbrain dopaminergic system, which leads to a deficit in sensorimotor gating (Yee et al., 2005). Of note, lack of GABA_Aα3 is not compensated by upregulation of other major GABA_A receptor subunits (i.e., GABA_Aα1, GABA_Aα2, GABA_Aβ2/3, or GABA_Aγ2) (Yee et al., 2005). Another brain region where GABA_Aα3 receptors are predominant is the nucleus reticularis thalami (Fritschy and Mohler, 1995; Pirker et al., 2000). Analyses of GABA_Aα3 deficiency in this region as well revealed that nucleus reticularis thalami neurons do not replace GABA_Aα3

with other GABA_A (α 1, α 2, or α 5) receptor types (Studer et al., 2006). In these neurons, GABA_A α 3 and GABA_A γ 2 are clustered together, similar to co-clustered GABA_A α 3- γ 2 receptors across ON α RGCs. In neurons of the nucleus reticularis thalami, lack of GABA_A α 3 leads to a disruption in GABA_A γ 2 clustering (Studer et al., 2006), similar to our observations of a severe attenuation in GABA_A γ 2 puncta across α 3KO ON α RGCs. In contrast, although GABA_A α 3 and GABA_A γ 2 deficiency impaired the clustering of gephyrin in α 3KO nucleus reticularis thalami neurons (Studer et al., 2006), the gephyrin distribution across α 3KO ON α RGCs remained unchanged in terms of both its distribution and its density. One possibility for this observation could be the very early expression of gephyrin across ON α RGCs compared with the timeline of GABA_A and GlyR expression. As gephyrin expression levels across the ON α reach mature levels as early as P8, it seems likely that gephyrin does not require the presence of either GABA_A or GlyR receptors for its postsynaptic localization and could be upstream to the role of GABA_A α 3 for the organization and formation of ON α inhibitory synapses. In contrast to gephyrin, however, GABA_A α 3 and GlyR expression levels along ON α dendrites reach mature levels around the time of eye opening, and GABA_A α 3 expression precedes emergence of GlyR α 1 receptors. Thus, early GABA_A α 3 might play an instructive role for the recruitment and clustering of GlyR α 1 at ON α mixed GABA_A α 3-GlyR α 1 synapses. Our observation that the proportion of GlyR α 1 lost in α 3KO ON α RGCs could represent the mixed GABA_A α 3-GlyR α 1 synapse fraction reaffirms this organizational role of early GABA_A α 3 receptors. Of note, the organizational role of GABA_A α 3 during retinal circuit assembly is circuit specific, as inhibitory microcircuits (containing mixed GABA_A α 3-GlyR α 1 synapses) impinging on the ON α RGC are selectively altered, and GlyR α 1 synapses distributed across other RGC types such as OFF RGCs are not impaired upon GABA_A α 3 deficiency. Future studies are necessary to delineate the functional consequences of lost mixed GABA_A α 3-GlyR α 1 synapses on the response properties of ON α RGCs.

ON-WACs as a presynaptic interneuronal partner to ON α RGCs

The ON-WACs reconstructed in our study provide inhibitory input onto the ON α predominantly at synapses with dual synaptic vesicle release sites. Interestingly, the glutamatergic (excitatory) input that the ON α RGC receives through type 6 bipolar cells (Schwartz et al., 2012) is at multisynaptic sites (Morgan et al., 2011), which could underlie the robust excitatory drive provided by type 6 bipolar cells to ON α RGCs (Schwartz et al., 2012). The input from ON-WAC multi-release sites onto ON α RGCs could thus represent the inhibitory counterpart to the type 6 bipolar cell->ON α excitatory synapse. Of note, thalamic afferents also use multi-release site presynaptic boutons for synapsing onto cortical interneurons to guarantee reliable transmission (Bagnall et al., 2011). Thus, the multi-release site appositions between the ON-WACs->ON α RGCs could be a “fail-safe” mechanism of synaptic inhibition.

The morphology of the ON-WAC resembles the type 53 AC type determined by Helmstaedter et al. (2013) during their connectomic reconstructions of the inner retina. The functional role of the ON-WAC remains to be determined, and future studies capitalizing on new AC transgenic lines would be needed to target this cell type for electrophysiology. Of note, a recent study profiling the AC population found ACs in the inner nuclear layer

positive for both the glycinergic AC marker glycine transporter-1 and the GABA synthetic enzyme (glutamic acid decarboxylase) (Yan et al., 2020). The ON-WAC profiles unveiled in our study do have somata in the inner nuclear layer and could thus likely be the same AC population as observed in the profiling study. Future studies are needed to find AC-specific transgenic lines that label ON-WACs and then perform immunolabeling to show that these cells are positive for both GABA and glycinergic markers.

Mixed synaptic circuits of the CNS (i.e., synapses using more than one neurotransmitter system) can use pre- or postsynaptic segregation or specialization mechanisms. Golgi-inhibitory interneurons of the cerebellar granular layer can mediate GABAergic inhibition of granule cells and glycinergic inhibition of unipolar brush cells because of the differential expression of GABARs and GlyRs in a target-specific manner and not by segregation of the inhibitory neurotransmitters across presynaptic terminals (Dugué et al., 2005). In contrast, the ON-WACs identified in our study could potentially use a model in which GABA and glycine are released at distinct sites along the presynaptic terminal boutons, as suggested by our EM observation of dual synaptic vesicle release sites of ON-WAC boutons. Other ACs have been reported to co-release different neurotransmitters: the starburst ACs co-release acetylcholine and GABA through distinct presynaptic vesicle pools (Lee et al., 2010), and the dopaminergic ACs co-release dopamine and GABA from synaptic vesicles that can express transporters for both neurotransmitters leading to co-enrichment and simultaneous release (Hirasawa et al., 2012). Given that the same vesicular transporter can enrich both GABA and glycine within presynaptic vesicles (Wojcik et al., 2006), future EM studies using postembedding immunogold labeling for the two inhibitory neurotransmitters are needed to determine if GABA-containing vesicles and glycine-containing vesicles are differentially enriched at segregated ON-WAC release sites. Thus, our results showing the presence of mixed GABA-glycine inhibitory circuits in the retina will motivate future studies that further explore the structural and functional properties of this motif of retinal inhibition and how it is recruited to support retinal processing.

STAR★METHODS

RESOURCE AVAILABILITY

Lead contact—Further information and requests for resources and reagents should be directed to and will be fulfilled by the Lead Contact, Mrinalini Hoon (mhoon@wisc.edu).

Materials availability—This study did not generate new unique reagents.

Data and code availability—The datasets supporting the current study have not been deposited in a public repository because of extremely large file sizes but are available from the Lead Contact on request.

EXPERIMENTAL MODEL AND SUBJECT DETAILS

All experiments were performed in accordance with the guidelines of the Institutional Animal Care and Use Committee of the University of Wisconsin-Madison and the National Institutes of Health. Animals of both sexes were used for experiments. *Thy1-YFPH* mice

(Bleckert et al., 2014; Feng et al., 2000) were used at P8, P12, P16, P21 and adult (> 1.5 months) time-points. This line was crossed into the GABA_Aα3 knockout transgenic line (Yee et al., 2005) and age-matched adult (> 1.5 month) littermate control and knockout animals were used for all the GABA_Aα3 knockout analyses. To visualize GABA_Aγ2 receptor sites across the RGC arbors, the *Thy1-YFPγ2* mice (Bleckert et al., 2013) were utilized and crossed into the GABA_Aα3 knockout background to assess GABA_Aγ2 puncta across RGCs in age-matched adult (> 1.5 month) littermate control and GABA_Aα3 knockout animals. For experiments involving biolistics, 1.2–1.5 month old *Thy1-GABA_Aγ2YFP* × GABA_Aα3 knockout and age-matched littermate control animals were used (Figure 7) and 1.2–1.5 month old age-matched GABA_Aα3 knockout-littermate control animals were used for PSD-95 transfections (Figure S7). All electrophysiology experiments were carried out on 1.5 month old wild-type animals (C57B6/J; Jackson Labs).

METHOD DETAILS

Immunohistochemistry—Animals were euthanized with Isoflurane, decapitated, and enucleated. Retinas were dissected in cold oxygenated mouse artificial cerebrospinal fluid (mACSF, pH 7.4) containing (in mM): 119 NaCl, 2.5 KCl, 2.5 CaCl₂, 1.3 MgCl₂, 1 NaH₂PO₄, 11 glucose, and 20 HEPES. During retina dissections note was taken of retinal location and orientation (Wei et al., 2010). Whole-mount immunolabelings were performed on retinas that were flattened on a filter paper (Millipore, HABP013). Flat-mounted retinas were fixed for 15 mins in 4% paraformaldehyde (in mACSF). After rinses in phosphate buffer (PBS), the retinas were pre-incubated in blocking solution containing 5% donkey serum and 0.5% Triton X-100 (in PBS) followed by incubation with primary antibodies in blocking solution over 3–4 nights at 4°C. Primary antibodies used were directed against: GFP (1:1000, chicken, Abcam), GABA_Aα3 (1:3000, guinea pig, J.M. Fritschy), GABA_Aα1 (1:5000, guinea pig, J.M. Fritschy), GlyRα1 (1:500, mouse monoclonal mAb2b, Synaptic Systems) and gephyrin (1:1000, mouse monoclonal clone 3B11, Synaptic systems). Secondary antibody incubation was carried out overnight in PBS using anti-isotypic Alexa Fluor (1:1000, Invitrogen) or DyLight conjugates (1:1000, Jackson ImmunoResearch). Retinas were subsequently mounted on slides using Vectashield mounting medium (Vector Labs).

Biolistic transfections—Gold particles (1.6 μm diameter, Bio-Rad) were coated with DNA plasmids encoding either tdTomato or postsynaptic density protein 95 fused to cyan fluorescent protein (PSD95-CFP) under the control of the cytomegalovirus (CMV) promoter (Bleckert et al., 2013; Okawa et al., 2019). The particles were biolistically delivered to whole-mount retinas using a Helios gene gun (Bio-Rad). Transfected retinas were subsequently incubated in mACSF solution in a humid oxygenated chamber at 33°C for a period of 24–26 hours. Post-incubation, retinas were fixed for 20 mins in 4% PFA and after washes in PBS were either mounted and coverslipped directly or processed for immunohistochemistry as described in the previous section.

Image acquisition and analysis—Image were acquired using a Leica laser scanning confocal microscope (Leica TCS LSP8), or an Olympus FV1000 confocal microscope. All image stacks were acquired using a 63x oil immersion objective (NA 1.4) with an

approximate voxel size of $0.1 \mu\text{m} \times 0.1 \mu\text{m} \times 0.4 \mu\text{m}$ (X-Y-Z resolution). Given the gradient in ON α RGC dendritic arbors across the nasal-temporal axis of the retina (Bleckert et al., 2014), these regions were avoided when collecting ON α RGC data across transgenic retinas to ensure comparable dendritic field sizes across the different retinas and genotypes. Raw images were subsequently median-filtered using ImageJ (FIJI, NIH) and visualized using Amira image analyses software (Thermo Fisher Scientific). For extracting synaptic signal specifically within ON α RGCs, the soma and dendrites of ON α RGCs were masked in 3D using the *LabelField* function in Amira. Thereafter the *Arithmetic* function was utilized to multiply a synaptic protein channel with the RGC mask.

For estimating colocalization between GlyR α 1 and GABA A α 3 puncta, the GlyR α 1 signal within the ON α RGC was first isolated and each individual puncta was masked in 3D to create regions of interest (ROIs) encompassing the entire puncta volume (across image planes). These delineated ROIs specifically marked GlyR α 1 receptor puncta volume in 3D within the ON α RGC. A custom written MATLAB code (Mathworks, USA) was thereafter used to ascertain colocalization between the demarcated GlyR α 1 puncta and the GABA A α 3 channel. The GABA A α 3 receptor channel was first thresholded as described in Hoon et al., 2017 and Sinha et al., 2017 to exclude any background (noise) signals. To threshold the GABA A α 3 signal, a plot of all GABA A α 3 pixels was considered and a threshold 3 standard deviations above the noise peak was selected (for more details see Hoon et al., 2017 and Sinha et al., 2017). The proportion of GlyR α 1 puncta (ROI) that also contained the thresholded GABA A α 3 signal within their 3D volume was next calculated. A GlyR α 1 puncta was deemed as “colocalized” if the thresholded GABA A α 3 signal occupied more than 20% volume of all pixels representing the GlyR α 1 punctum. Analyzing the proportion of GlyR α 1 ROI that were colocalized (i.e., volume overlap with GABA A α 3) yielded a % colocalization. To assess random interactions, the GABA A α 3 channel was flipped 90 degrees and a % colocalization determination was made similar to the procedure outlined above (see also Sinha et al., 2017 for additional details). As our analyses routine considers the entire 3D volume of the GlyR α 1 we are also accounting for scenarios where the two receptor puncta are offset and incorporates postsynaptic scenarios where the GABA A α 3 and GlyR α 1 clusters are partially overlapping and apposed to dual release presynapses as observed in the ON α electron microscopy data and synaptic arrangements shown in scenarios III-IV (Figure 2A).

For estimation of % receptor occupancies across the dendritic arbors of ON α RGCs, the dendrites of the RGCs were masked in 3D using Amira and multiplied with the receptor channel to isolate the receptor signal within the RGC dendrites (as described above). A threshold was thereafter applied to the receptor channel (3 standard deviations above the channel noise peak, see Hoon et al., 2017; Sinha et al., 2017 for more details) to eliminate background noise pixels and quantify volume of ‘detected’ receptor pixels within the RGC dendritic mask. The volume of the receptor pixels was expressed relative to the RGC dendritic volume for determination of the % receptor occupancy. This method ensured normalization across RGC dendritic sizes.

For quantifying the number of synaptic puncta within the soma and dendrites of ON α RGCs, the soma and dendrites of an individual ON α RGC were at first masked out (using

Amira as described above) and the synaptic channel signal specifically within these structures was isolated. ROIs delineating each receptor cluster (puncta) were thereafter generated for the clusters along the ON α RGC dendrite and within the soma. These masks were imported into MATLAB and a custom written code extracted the soma centroid location, total dendritic volume, puncta size, puncta number, and puncta centroid location. Receptor puncta within soma or dendrite were thereafter ascertained to calculate puncta number and density estimates.

Electron microscopy—The *Thy1-YFP* line was used to visualize the ON α RGC for branding its location with fiduciary marks using the technique of Near-infrared branding (NIRB) (Bishop et al., 2011; Bleckert et al., 2013). The retina was processed for generating electron microscopy blocs using the protocol and steps outlined in Della Santina et al., 2016. Fiduciary marks were used to identify the location of the ON α RGC at the electron microscope level. A Zeiss 3 View serial block face scanning electron microscope was used to image the retinal region with the ON α RGC in a 3 \times 2 montage (tiles approximately 50 \times 50 μ m; 8000 \times 8000 pixels per tile and z section thickness of 50nm) centered on the NIRBed ON α RGC to capture the soma and the proximal dendritic arbors. Image stacks were visualized and aligned using TrakEM2 plugin of Fiji (ImageJ, NIH). The ON α RGC was reconstructed and all inhibitory synapses annotated to determine distribution of these sites across the proximal dendritic arbor. Amira was used for visualization and display. For analyses of the synaptic distribution across a wider dendritic field of an ON α RGC and for tracing of connected presynaptic partners, the k0725 dataset was obtained through the Briggman Lab (courtesy of Dr. Kevin Briggman) and visualized using the KNOSSOS software (*Max Planck Institute for Medical Research* in Heidelberg, Germany). Skeletons of cells were exported into Amira using MATLAB codes from the Briggman Lab and locations of soma and synapses were depicted as spheres. Acquisition parameters and sample preparation details of the k0725 dataset is described in Ding et al., 2016.

In the k0725 dataset, the ON α RGC was identified by its characteristic dendritic lamination in the retinal inner plexiform layer. This was done by masking potential RGCs and comparing their dendritic lamination with skeletons of ON Starburst ACs (SACs) provided by the Briggman lab (Ding et al., 2016) as ON α RGC dendrites should laminate below the ON SAC arbors (Krieger et al., 2017). Only one ON α RGC was thus identified based on our criterion. As the soma of this cell was not completely within the boundaries of the dataset, synaptic information for the cell was acquired from analyses of all of its dendritic arbors within the volume of the stack.

Inhibitory synapses were identified by the presence of a pool of synaptic vesicles clustered along a release site and apposed to a thickened pre- and postsynaptic membranes as previously described (Gray, 1969). Synapses were only confirmed when 2–3 consecutive image planes displayed these ultrastructural features. Single and multiple release sites were confirmed by scrutinizing synaptic vesicle clustering across 2–3 consecutive image planes. The synaptic distribution was ascertained by this analysis procedure for both the NIRBed ON α RGC as well as the ON α RGC arbors in the k0725 dataset. Presynaptic boutons with multiple release sites resembled the ultrastructure of thalamic afferents->cortical interneuron synapses (Bagnall et al., 2011). To quantify the distance between two vesicle clusters in a

multi-release presynaptic bouton, we quantified the distance between the centers of the two vesicle pools and averaged this measure across 2–3 consecutive image planes. On average two vesicle clusters in a multi-release ON-WAC bouton were separated by a distance of 319.30 ± 24.73 nm ($n = 58$ boutons with dual release sites). Synapses were classified by number of release sites into single or multiple (dual, triple or quadruple) and these categories were non-overlapping. To measure bouton diameter, the EM planes with the largest bouton diameter were considered and for each bouton a diameter average across 2–3 consecutive image planes was calculated.

For identifying and tracing presynaptic amacrine partners in the k0725 dataset, starkly visible (most-prominent) dual release site-containing amacrine boutons were traced to identify and mask presynaptic amacrine interneurons/partners. Upon identification of 3 Widefield ON-laminating Amacrine Cells (ON-WACs), total inhibitory output onto the ON α RGC from each interneuron was quantified using the same procedure as described above. We also determined the output (inhibitory synapses) made by the ON-WACs onto other (non-ON α) ganglion cells, amacrine cell processes and bipolar cell terminals. Retinal bipolar cell terminals were characterized by presence of ribbon sites, amacrine processes were characterized by presence of inhibitory output synapses and ganglion cell processes were determined by presence of large microtubule-filled dendrites that lack output synapses or accumulation of synaptic vesicles similar to criteria detailed in Gamlin et al. (2020).

Patch-clamp electrophysiology—Retinae from light-adapted wild-type mice were used for electrophysiology experiments. Isolated retina was stored in oxygenated (95% O₂/5% CO₂) Ames medium (Sigma-Aldrich, St. Louis, MO) at ~30°C. Isolated retinas were flattened onto poly-l-lysine slides (Sinha et al., 2016), placed in a upright microscope, and perfused with oxygenated Ames solution at a rate of ~5 mL/min. During recordings, retinal neurons were visualized and targeted using infrared illumination (940 nm, Sutter Instrument). ON α RGCs, were targeted based on their relatively big soma size and their light-evoked response characteristics assessed by cell-attached spike recordings (Figures S3A and S3B). A full-field light stimuli (diameter 450 μ m) was delivered to the tissue from an LED with peak spectral output at 505 nm at an intensity that caused isomerization of ~1000 opsin molecules per cone per second. Electrophysiological recordings were performed using a MultiClamp 700B amplifier (Molecular Devices) by fire polished borosilicate glass pipettes (3–5 MU; Sutter Instrument) pulled using a DMZ-Zeitz puller (Zeitz Instruments). All voltage traces were sampled at 50 kHz and low pass filtered at 3 kHz. All electrophysiology data were acquired by a MATLAB-based data acquisition software (Symphony-DAS). Voltage-clamp recordings were obtained using pipettes filled with an intracellular solution containing (in mM) the following: 105 CsCH₃SO₃, 10 TEA-Cl, 20 HEPES, 10 EGTA, 2 QX-314, 5 Mg-ATP, 0.5 Tris-GTP (~280 mOsm; pH ~7.3 with CsOH). Alexa 594 dye (100–200 microM) was included in the intracellular solution to image the ganglion cells post recording as shown in Figure 2B. Miniature inhibitory postsynaptic currents (mIPSCs) were isolated by including blockers for glutamate receptors - 5 μ M NBQX (2,3-Dioxo-6-nitro-1,2,3,4-tetrahydrobenzo[*f*]quinoxaline-7-sulfonamide disodium salt - AMPA receptor antagonist) and 50 μ M D-AP5 (D-(-)-2-Amino-5-phosphonopentanoic acid – competitive NMDA antagonist) together with 0.1 μ M TTX

(Tetrodotoxin – voltage-gated sodium channel blocker), in the Ames solution. For sIPSC recordings, TTX was excluded from the excitatory blocker cocktail. Inhibitory postsynaptic current measurements were made before and after the application of 20 μ M GABAzine (selective GABA_A receptor blocker) or 2 μ M Strychnine (Glycine receptor antagonist). mIPSCs and sIPSCs were detected using a built-in event detection routine in the Neuromatic software (Rothman and Silver, 2018). Events were then analyzed for estimating kinetics, frequency, and amplitude of m/sIPSCs using Neuromatic and self-written routines in Igor Pro (Wavemetrics, USA) and MATLAB (Mathworks, USA). mIPSC recordings were performed at a membrane potential of -70 mV where the inhibitory synaptic currents appear as inward currents. sIPSC recordings were performed at a membrane potential of 10 mV where the inhibitory synaptic currents appear as outward currents. We verified that decay kinetics of sIPSCs are slower at room temperature (Average \pm SEM for decay time of sIPSC events from 5 ON α RGCs = 2.89 ± 0.37) compared to recordings at physiological temperatures ($\sim 30^{\circ}\text{C}$; decay time distribution in Figure S3; Average \pm SEM = 1.778 ± 0.164) as suggested for mouse retinal alpha ganglion cells by Majumdar et al., 2007 (Majumdar et al., 2007).

QUANTIFICATION AND STATISTICAL ANALYSIS

Statistical details of experiments and comparative analyses including number of cells/ animals analyzed and tests utilized is provided in the Figure legends. Unless otherwise stated plotted graphs represent mean \pm SEM values.

Supplementary Material

Refer to Web version on PubMed Central for supplementary material.

ACKNOWLEDGMENTS

We would like to acknowledge Dr. Kevin Briggman and the Briggman lab for sharing the k0725 dataset and for generously providing us with MATLAB codes to enable visualization of the EM reconstructions. This work was supported by NIH grants EY031677 (to M.H.), EY10699 (to Rachel Wong and support for A.B., C.G., and W.-Q.Y.), EY026070 (to R.S.), Vision Research Core grant EY01730 (to M. Neitz), T32HD007183 and EY07031 (to C.G.), the McPherson Eye Research Institute's Professorship (to R.S. and M.H.), and an unrestricted grant from Research to Prevent Blindness to the University of Wisconsin (UW)-Madison Department of Ophthalmology. We are grateful to J.M. Fritschy for generously providing antibodies towards specific GABA_A receptors. We are thankful to E. Parker for expert technical assistance.

REFERENCES

- Antinucci P, and Hindges R (2018). Orientation-selective retinal circuits in vertebrates. *Front. Neural Circuits* 12, 11. [PubMed: 29467629]
- Baden T, Berens P, Franke K, Román Rosón M, Bethge M, and Euler T (2016). The functional diversity of retinal ganglion cells in the mouse. *Nature* 529, 345–350. [PubMed: 26735013]
- Bagnall MW, Hull C, Bushong EA, Ellisman MH, and Scanziani M (2011). Multiple clusters of release sites formed by individual thalamic afferents onto cortical interneurons ensure reliable transmission. *Neuron* 71, 180–194. [PubMed: 21745647]
- Bishop D, Niki I, Brinkoetter M, Knecht S, Potz S, Kerschensteiner M, and Misgeld T (2011). Near-infrared branding efficiently correlates light and electron microscopy. *Nat. Methods* 8, 568–570. [PubMed: 21642966]

- Bleckert A, Parker ED, Kang Y, Pancaroglu R, Soto F, Lewis R, Craig AM, and Wong RO (2013). Spatial relationships between GABAergic and glutamatergic synapses on the dendrites of distinct types of mouse retinal ganglion cells across development. *PLoS ONE* 8, e69612. [PubMed: 23922756]
- Bleckert A, Schwartz GW, Turner MH, Rieke F, and Wong RO (2014). Visual space is represented by nonmatching topographies of distinct mouse retinal ganglion cell types. *Curr. Biol* 24, 310–315. [PubMed: 24440397]
- Bosman LW, Rosahl TW, and Brussaard AB (2002). Neonatal development of the rat visual cortex: synaptic function of GABAA receptor alpha subunits. *J. Physiol* 545, 169–181. [PubMed: 12433958]
- Cao LH, Yang D, Wu W, Zeng X, Jing BY, Li MT, Qin S, Tang C, Tu Y, and Luo DG (2017). Odor-evoked inhibition of olfactory sensory neurons drives olfactory perception in *Drosophila*. *Nat. Commun* 8, 1357. [PubMed: 29116083]
- Della Santina L, Kuo SP, Yoshimatsu T, Okawa H, Suzuki SC, Hoon M, Tsuboyama K, Rieke F, and Wong ROL (2016). Glutamatergic monopolar interneurons provide a novel pathway of excitation in the mouse retina. *Curr. Biol* 26, 2070–2077. [PubMed: 27426514]
- Ding H, Smith RG, Poleg-Polsky A, Diamond JS, and Briggman KL (2016). Species-specific wiring for direction selectivity in the mammalian retina. *Nature* 535, 105–110. [PubMed: 27350241]
- Dugué GP, Dumoulin A, Triller A, and Dieudonné S (2005). Target-dependent use of co-released inhibitory transmitters at central synapses. *J. Neurosci* 25, 6490–6498. [PubMed: 16014710]
- Feng G, Mellor RH, Bernstein M, Keller-Peck C, Nguyen QT, Wallace M, Nerbonne JM, Lichtman JW, and Sanes JR (2000). Imaging neuronal subsets in transgenic mice expressing multiple spectral variants of GFP. *Neuron* 28, 41–51. [PubMed: 11086982]
- Frazao R, Nogueira MI, and Wässle H (2007). Colocalization of synaptic GABA(C)-receptors with GABA (A)-receptors and glycine-receptors in the rodent central nervous system. *Cell Tissue Res* 330, 1–15. [PubMed: 17610086]
- Fritschy JM, and Mohler H (1995). GABAA-receptor heterogeneity in the adult rat brain: differential regional and cellular distribution of seven major subunits. *J. Comp. Neurol* 359, 154–194. [PubMed: 8557845]
- Gamlin CR, Yu WQ, Wong ROL, and Hoon M (2018). Assembly and maintenance of GABAergic and Glycinergic circuits in the mammalian nervous system. *Neural Dev* 13, 12. [PubMed: 29875009]
- Gamlin CR, Zhang C, Dyer MA, and Wong ROL (2020). Distinct developmental mechanisms act independently to shape biased synaptic divergence from an inhibitory neuron. *Curr. Biol* 30, 1258–1268.e2. [PubMed: 32109390]
- Gray EG (1969). Electron microscopy of excitatory and inhibitory synapses: a brief review. *Prog. Brain Res* 31, 141–155. [PubMed: 4899407]
- Greferath U, Grünert U, Fritschy JM, Stephenson A, Möhler H, and Wässle H (1995). GABAA receptor subunits have differential distributions in the rat retina: in situ hybridization and immunohistochemistry. *J. Comp. Neurol* 353, 553–571. [PubMed: 7759615]
- Grimes WN, Schwartz GW, and Rieke F (2014). The synaptic and circuit mechanisms underlying a change in spatial encoding in the retina. *Neuron* 82, 460–473. [PubMed: 24742466]
- Haverkamp S, and Wässle H (2000). Immunocytochemical analysis of the mouse retina. *J. Comp. Neurol* 424, 1–23. [PubMed: 10888735]
- Helmstaedter M, Briggman KL, Turaga SC, Jain V, Seung HS, and Denk W (2013). Connectomic reconstruction of the inner plexiform layer in the mouse retina. *Nature* 500, 168–174. [PubMed: 23925239]
- Hirasawa H, Betensky RA, and Raviola E (2012). Corelease of dopamine and GABA by a retinal dopaminergic neuron. *J. Neurosci* 32, 13281–13291. [PubMed: 22993444]
- Hoon M, Okawa H, Della Santina L, and Wong RO (2014). Functional architecture of the retina: development and disease. *Prog. Retin. Eye Res* 42, 44–84. [PubMed: 24984227]
- Hoon M, Sinha R, and Okawa H (2017). Using fluorescent markers to estimate synaptic connectivity in situ. *Methods Mol. Biol* 1538, 293–320. [PubMed: 27943198]
- Isaacson JS, and Scanziani M (2011). How inhibition shapes cortical activity. *Neuron* 72, 231–243. [PubMed: 22017986]

- Jonas P, Bischofberger J, and Sandkühler J (1998). Corelease of two fast neurotransmitters at a central synapse. *Science* 281, 419–424. [PubMed: 9665886]
- Kerschensteiner D, Morgan JL, Parker ED, Lewis RM, and Wong RO (2009). Neurotransmission selectively regulates synapse formation in parallel circuits in vivo. *Nature* 460, 1016–1020. [PubMed: 19693082]
- Koulen P, Sassoè-Pognetto M, Grünert U, and Wässle H (1996). Selective clustering of GABA(A) and glycine receptors in the mammalian retina. *J. Neurosci* 16, 2127–2140. [PubMed: 8604056]
- Krieger B, Qiao M, Rouso DL, Sanes JR, and Meister M (2017). Four alpha ganglion cell types in mouse retina: function, structure, and molecular signatures. *PLoS ONE* 12, e0180091. [PubMed: 28753612]
- Kuo SP, Bradley LA, and Trussell LO (2009). Heterogeneous kinetics and pharmacology of synaptic inhibition in the chick auditory brainstem. *J. Neurosci* 29, 9625–9634. [PubMed: 19641125]
- Laurie DJ, Wisden W, and Seeburg PH (1992). The distribution of thirteen GABAA receptor subunit mRNAs in the rat brain. III. Embryonic and postnatal development. *J. Neurosci* 12, 4151–4172. [PubMed: 1331359]
- Lee S, Kim K, and Zhou ZJ (2010). Role of ACh-GABA cotransmission in detecting image motion and motion direction. *Neuron* 68, 1159–1172. [PubMed: 21172616]
- Lee SC, Meyer A, Schubert T, Hüser L, Dedek K, and Haverkamp S (2015). Morphology and connectivity of the small bistratified A8 amacrine cell in the mouse retina. *J. Comp. Neurol* 523, 1529–1547. [PubMed: 25630271]
- Liu Q, and Wong-Riley MT (2004). Developmental changes in the expression of GABAA receptor subunits alpha1, alpha2, and alpha3 in the rat pre-Botzinger complex. *J. Appl. Physiol.* (1985) 96, 1825–1831. [PubMed: 14729731]
- Lu T, Rubio ME, and Trussell LO (2008). Glycinergic transmission shaped by the corelease of GABA in a mammalian auditory synapse. *Neuron* 57, 524–535. [PubMed: 18304482]
- MacNeil MA, and Masland RH (1998). Extreme diversity among amacrine cells: implications for function. *Neuron* 20, 971–982. [PubMed: 9620701]
- Majumdar S, Heinze L, Haverkamp S, Ivanova E, and Wässle H (2007). Glycine receptors of A-type ganglion cells of the mouse retina. *Vis. Neurosci* 24, 471–487. [PubMed: 17550639]
- Masland RH (1988). Amacrine cells. *Trends Neurosci* 11, 405–410. [PubMed: 2469207]
- McKernan RM, and Whiting PJ (1996). Which GABAA-receptor subtypes really occur in the brain? *Trends Neurosci* 19, 139–143. [PubMed: 8658597]
- Morgan JL, Schubert T, and Wong RO (2008). Developmental patterning of glutamatergic synapses onto retinal ganglion cells. *Neural Dev* 3, 8. [PubMed: 18366789]
- Morgan JL, Soto F, Wong RO, and Kerschensteiner D (2011). Development of cell type-specific connectivity patterns of converging excitatory axons in the retina. *Neuron* 71, 1014–1021. [PubMed: 21943599]
- Münch TA, da Silveira RA, Siebert S, Viney TJ, Awatramani GB, and Roska B (2009). Approach sensitivity in the retina processed by a multifunctional neural circuit. *Nat. Neurosci* 12, 1308–1316. [PubMed: 19734895]
- Murphy GJ, and Rieke F (2006). Network variability limits stimulus-evoked spike timing precision in retinal ganglion cells. *Neuron* 52, 511–524. [PubMed: 17088216]
- Nirenberg S, and Meister M (1997). The light response of retinal ganglion cells is truncated by a displaced amacrine circuit. *Neuron* 18, 637–650. [PubMed: 9136772]
- Okawa H, Yu WQ, Matti U, Schwarz K, Odermatt B, Zhong H, Tsukamoto Y, Lagnado L, Rieke F, Schmitz F, and Wong ROL (2019). Dynamic assembly of ribbon synapses and circuit maintenance in a vertebrate sensory system. *Nat. Commun* 10, 2167. [PubMed: 31092821]
- Park SJH, Pottackal J, Ke JB, Jun NY, Rahmani P, Kim IJ, Singer JH, and Demb JB (2018). Convergence and divergence of CRH amacrine cells in mouse retinal circuitry. *J. Neurosci* 38, 3753–3766. [PubMed: 29572434]
- Pirker S, Schwarzer C, Wieselthaler A, Sieghart W, and Sperk G (2000). GABA(A) receptors: immunocytochemical distribution of 13 subunits in the adult rat brain. *Neuroscience* 101, 815–850. [PubMed: 11113332]

- Rothman JS, and Silver RA (2018). NeuroMatic: an integrated open-source software toolkit for acquisition, analysis and simulation of electrophysiological data. *Front. Neuroinform* 12, 14. [PubMed: 29670519]
- Russier M, Kopysova IL, Ankri N, Ferrand N, and Debanne D (2002). GABA and glycine co-release optimizes functional inhibition in rat brainstem motoneurons in vitro. *J. Physiol* 541, 123–137. [PubMed: 12015425]
- Sanes JR, and Masland RH (2015). The types of retinal ganglion cells: current status and implications for neuronal classification. *Annu. Rev. Neurosci* 38, 221–246. [PubMed: 25897874]
- Sassoè-Pognetto M, and Wässle H (1997). Synaptogenesis in the rat retina: subcellular localization of glycine receptors, GABA(A) receptors, and the anchoring protein gephyrin. *J. Comp. Neurol* 381, 158–174. [PubMed: 9130666]
- Sassoè-Pognetto M, Kirsch J, Grünert U, Greferath U, Fritschy JM, Möhler H, Betz H, and Wässle H (1995). Colocalization of gephyrin and GABAA-receptor subunits in the rat retina. *J. Comp. Neurol* 357, 1–14. [PubMed: 7673460]
- Schwartz GW, Okawa H, Dunn FA, Morgan JL, Kerschensteiner D, Wong RO, and Rieke F (2012). The spatial structure of a nonlinear receptive field. *Nat. Neurosci* 15, 1572–1580. [PubMed: 23001060]
- Sinha R, Lee A, Rieke F, and Haeseleer F (2016). Lack of CaBP1/caldendrin or CaBP2 leads to altered ganglion cell responses. *eNeuro* 3, ENEURO.0099–16.2016.
- Sinha R, Hoon M, Baudin J, Okawa H, Wong ROL, and Rieke F (2017). Cellular and circuit mechanisms shaping the perceptual properties of the primate fovea. *Cell* 168, 413–426.e12. [PubMed: 28129540]
- Smeds L, Takeshita D, Turunen T, Tiihonen J, Westö J, Martyniuk N, Seppänen A, and Ala-Laurila P (2019). Paradoxical rules of spike train decoding revealed at the sensitivity limit of vision. *Neuron* 104, 576–587.e11. [PubMed: 31519460]
- Studer R, von Boehmer L, Haenggi T, Schweizer C, Benke D, Rudolph U, and Fritschy JM (2006). Alteration of GABAergic synapses and gephyrin clusters in the thalamic reticular nucleus of GABAA receptor alpha3 subunitnull mice. *Eur. J. Neurosci* 24, 1307–1315. [PubMed: 16987218]
- Thomson AM, and Jovanovic JN (2010). Mechanisms underlying synapse-specific clustering of GABA(A) receptors. *Eur. J. Neurosci* 31, 2193–2203. [PubMed: 20550567]
- Todd AJ, Watt C, Spike RC, and Sieghart W (1996). Colocalization of GABA, glycine, and their receptors at synapses in the rat spinal cord. *J. Neurosci* 16, 974–982. [PubMed: 8558266]
- van Wyk M, Wässle H, and Taylor WR (2009). Receptive field properties of ON- and OFF-ganglion cells in the mouse retina. *Vis. Neurosci* 26, 297–308. [PubMed: 19602302]
- Völgyi B, Chheda S, and Bloomfield SA (2009). Tracer coupling patterns of the ganglion cell subtypes in the mouse retina. *J. Comp. Neurol* 512, 664–687. [PubMed: 19051243]
- Wässle H (2004). Parallel processing in the mammalian retina. *Nat. Rev. Neurosci* 5, 747–757. [PubMed: 15378035]
- Wässle H, Koulen P, Brandstätter JH, Fletcher EL, and Becker CM (1998). Glycine and GABA receptors in the mammalian retina. *Vision Res* 38, 1411–1430. [PubMed: 9667008]
- Wässle H, Heinze L, Ivanova E, Majumdar S, Weiss J, Harvey RJ, and Haverkamp S (2009). Glycinergic transmission in the mammalian retina. *Front. Mol. Neurosci* 2, 6. [PubMed: 19924257]
- Wei W, and Feller MB (2011). Organization and development of direction-selective circuits in the retina. *Trends Neurosci* 34, 638–645. [PubMed: 21872944]
- Wei W, Elstrott J, and Feller MB (2010). Two-photon targeted recording of GFP-expressing neurons for light responses and live-cell imaging in the mouse retina. *Nat. Protoc* 5, 1347–1352. [PubMed: 20595962]
- Wojcik SM, Katsurabayashi S, Guillemain I, Friauf E, Rosenmund C, Brose N, and Rhee JS (2006). A shared vesicular carrier allows synaptic corelease of GABA and glycine. *Neuron* 50, 575–587. [PubMed: 16701208]
- Yan W, Laboulaye MA, Tran NM, Whitney IE, Benhar I, and Sanes JR (2020). Mouse retinal cell atlas: molecular identification of over sixty amacrine cell types. *J. Neurosci* 40, 5177–5195. [PubMed: 32457074]

- Yee BK, Keist R, von Boehmer L, Studer R, Benke D, Hagenbuch N, Dong Y, Malenka RC, Fritschy JM, Bluethmann H, et al. (2005). A schizophrenia-related sensorimotor deficit links alpha 3-containing GABAA receptors to a dopamine hyperfunction. *Proc. Natl. Acad. Sci. U S A* 102, 17154–17159. [PubMed: 16284244]
- Zhang C, and McCall MA (2012). Receptor targets of amacrine cells. *Vis. Neurosci* 29, 11–29. [PubMed: 22310370]
- Zhang C, Rompani SB, Roska B, and McCall MA (2014). Adeno-associated virus-RNAi of GlyR α 1 and characterization of its synapse-specific inhibition in OFF alpha transient retinal ganglion cells. *J. Neurophysiol* 112, 3125– 3137. [PubMed: 25231618]

Highlights

- Mixed GABA-glycine synapses are present across ON-sustained ganglion cell dendrites
- GABA and glycine are not co-released from the same presynaptic vesicle
- Widefield amacrine cells synapse with ON-sustained dendrites at dual release sites
- Early expression of GABA receptors recruits glycine receptors at mixed synapses

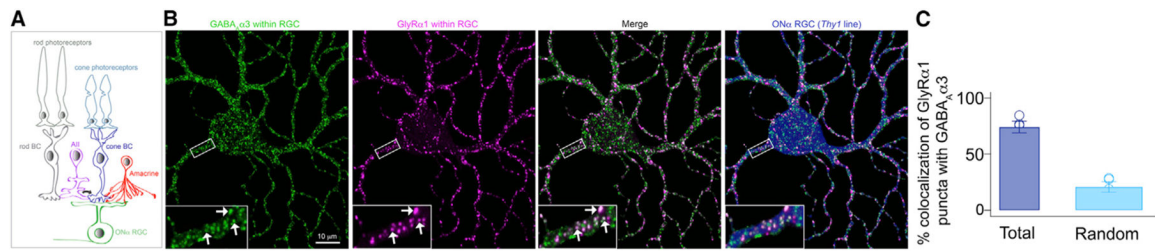


Figure 1. Mixed GABA-glycine receptor postsynapses are localized across ON α dendrites
 (A) Schematic of neural organization in mouse retina. Dim- and bright-light signals are sensed by rod and cone photoreceptors, which synapse onto rod and cone bipolar cells (BCs). Cone BCs provide direct excitatory input to ON α RGC at the inner plexiform layer, but rod BC signals are ferried to ON α RGC through AII interneurons. The ON α RGC receives inhibitory input from GABA and glycinergic amacrine cells (amacrine).
 (B) GABA α 3 (green) and GlyRa1 (magenta) receptor puncta within ON α RGC soma and proximal dendrites (blue) as visualized in the *Thy1-YFP* line. Inset shows higher magnification view of selected dendritic segment. White arrows point to three examples of colocalized GABA α 3 and GlyRa1 puncta.
 (C) Percentage colocalization of GlyRa1 puncta within ON α and GABA α 3 receptors. The random estimate was generated by flipping the GABA α 3 receptor channel 90° (n = 4 ON α RGCs from three retinas and three animals).

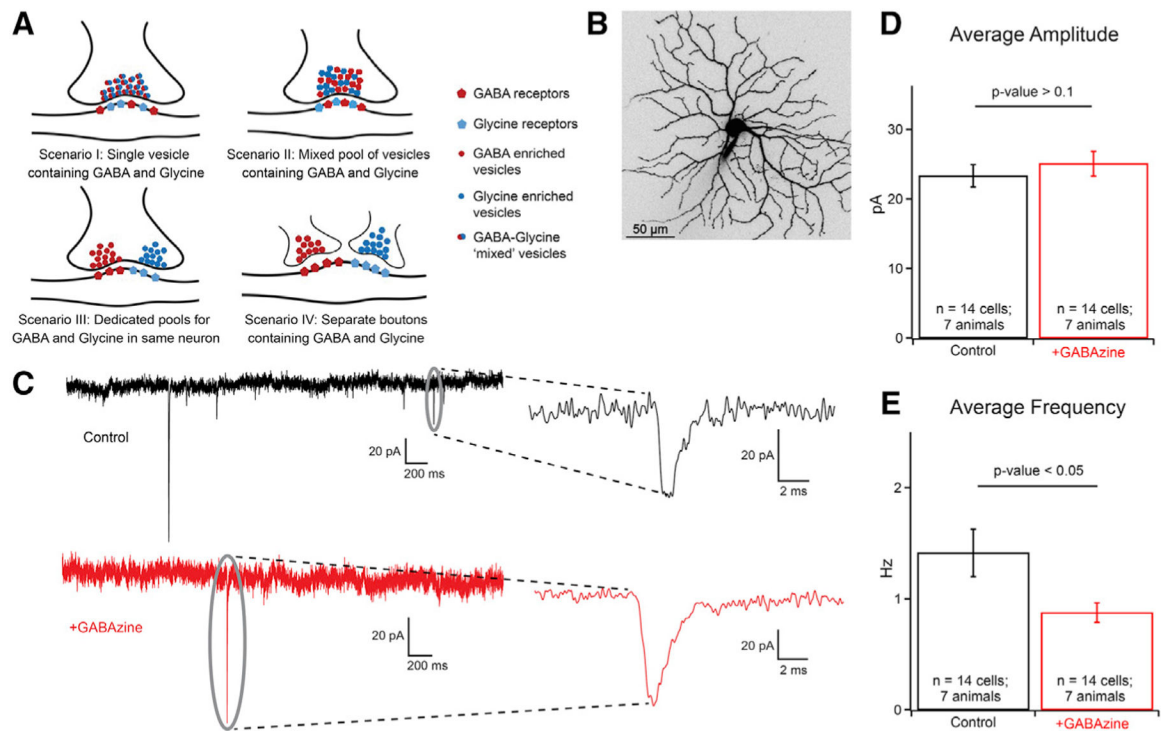


Figure 2. GABA and glycine are not co-released from the same presynaptic release vesicle onto ON α RGCs

(A) Different scenarios as to how “mixed” GABA-glycine synapses could be organized.

(B) An ON α RGC targeted for single-cell electrophysiology and filled with Alexa 594.

(C) Exemplar traces of miniature inhibitory postsynaptic currents (mIPSCs) recorded from ON α in the presence of NBQX, D-APV, and TTX (control; black trace) and after application of GABAzine (red trace).

(D) Quantification of mIPSC amplitude in control condition and after application of GABAzine.

(E) Quantification of occurrence (frequency) of mIPSCs in control condition and after application of GABAzine. A significant reduction in mIPSC frequency ($p = 0.0144$) was observed.

A paired two-tailed t test was performed for (D) and (E).

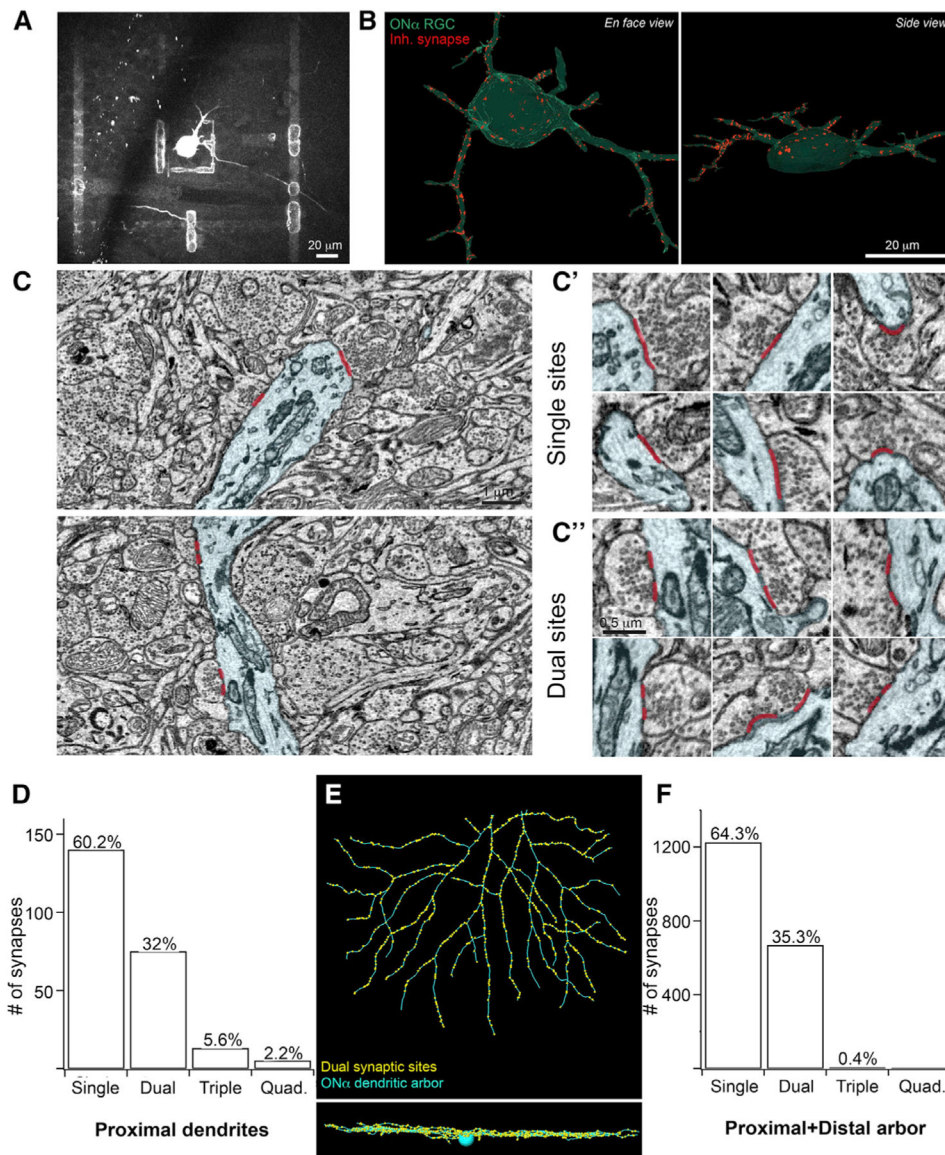


Figure 3. Inhibitory input with dual synaptic vesicle release sites uncovered by SBFSEM of inhibitory synapses across ON α RGCs

(A) An ON α in the *Thy1-YFPH* transgenic line after burning of fiduciary marks to locate and reconstruct the cell by SBFSEM.

(B) Three-dimensional (3D) reconstruction of the ON α RGC and proximal dendritic arbor (RGC, cyan-green) with annotated sites of inhibitory synaptic inputs (Inh synapse, red).

(C) Exemplar sections from a region of the ON α dendrite (cyan) with annotated inhibitory synapses containing single (top image) and dual (bottom image) release sites.

(D) (C' and C'') Magnified view of inhibitory synapses on the ON α arbor (cyan) with single (C') and dual (C'') synaptic vesicle release sites. Each synaptic vesicle release site is demarcated with a red line.

(E) Distribution of inhibitory synapses across the ON α as sorted into synapses with single, dual, triple, and quadruple release sites. This distribution was determined from the NIRBed ON α RGC.

(E) Top-down view of the dendritic arbor of an ON α RGC (cyan, reconstructed from k0725 dataset) with all dual synaptic vesicle release sites annotated (yellow). The bottom panel shows a side profile of the ON α with dual inhibitory synaptic sites distributed across both the proximal and distal dendritic arbor.

(F) Distribution of inhibitory synapses across the entire dendritic arbor of the ON α as sorted into synapses with single, dual, triple, and quadruple release sites. This distribution was determined from the ON α reconstructed from the k0725 dataset from Ding et al. (2016).

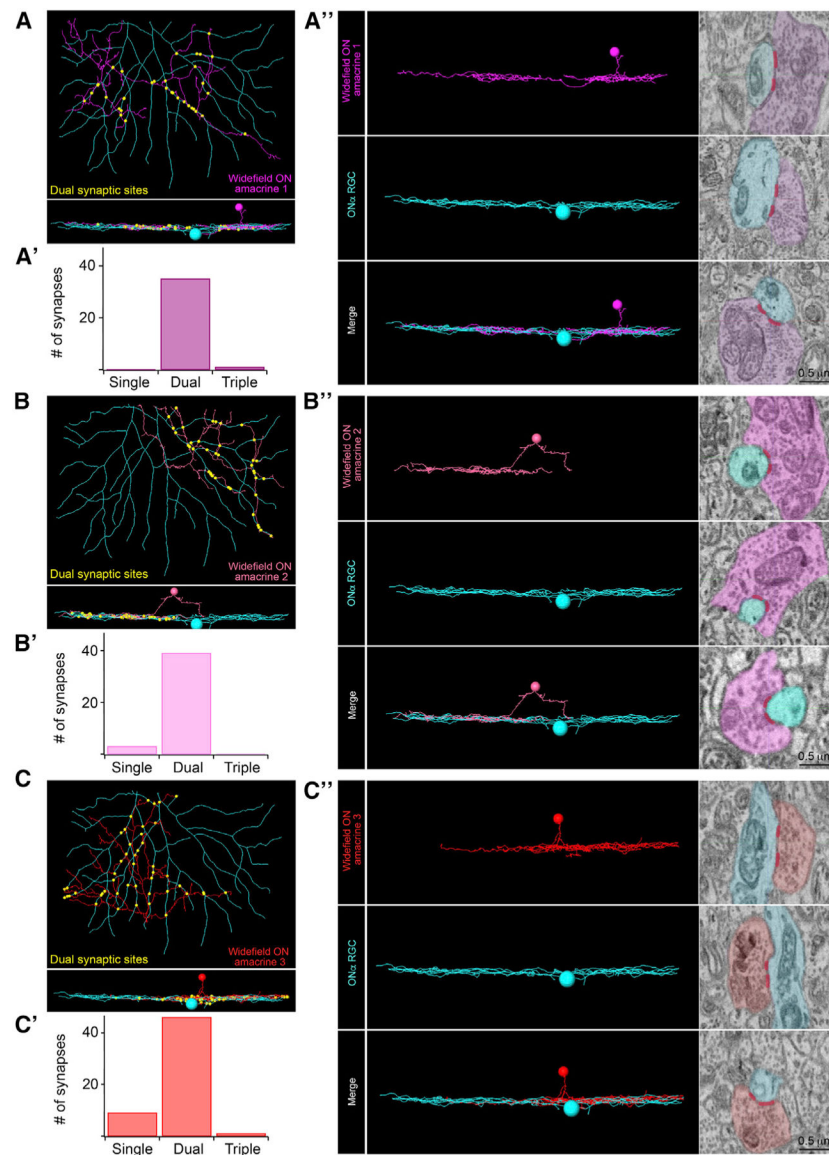


Figure 4. ON-laminating widefield amacrine cells provide inhibitory input onto ON α dendrites primarily at dual release sites

(A–C) Top-down view of SBFSEM reconstructions of three widefield ON-laminating amacrine cells that provide input onto the ON α dendritic arbor (cyan) at dual synaptic vesicle release sites (yellow). Widefield ON amacrine 1, magenta (A); widefield ON amacrine 2, pink (B); widefield ON amacrine 3, red (C). Bottom panels represent side profile of the amacrine neuron and ON α with dual synaptic sites annotated.

(A'–C') Distribution of the number of synapses with single, dual, or triple vesicle release sites the respective widefield ON amacrine cell makes onto the ON α dendritic arbor.

(A''–C'') Three-dimensional (3D) reconstruction of the widefield ON amacrine cell and the ON α RGC with three example raw EM images demonstrating inhibitory synaptic contact between the respective amacrine and ON α RGC at synapses with two synaptic vesicle release sites. Each synaptic vesicle release site is demarcated with a red line.

All reconstructions performed on the k0725 dataset from Ding et al. (2016).

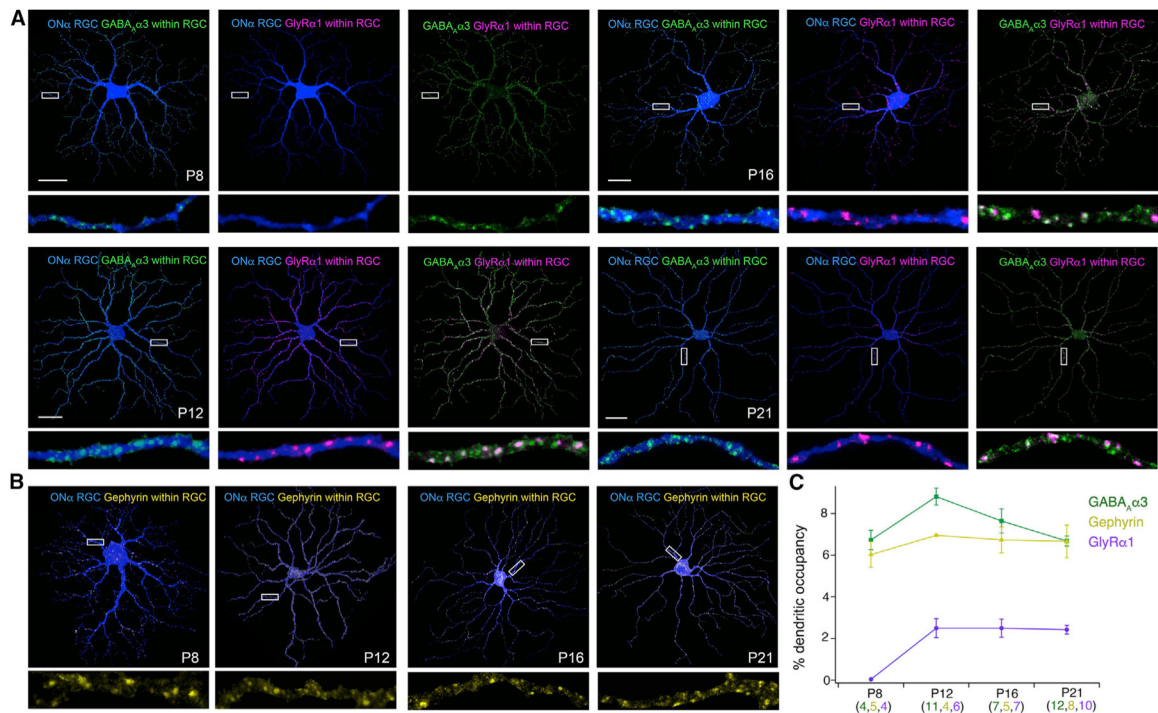


Figure 5. GABAergic synapses are established before glycinergic synapses on the ON α RGC dendritic arbor

(A) ON α RGC co-labeling with GABA_A α 3 and GlyR α 1 across time points in the *Thy1*-YFP line (P, postnatal day). GABA_A α 3 (green) and GlyR α 1 (magenta) signal within the RGC is overlaid on the RGC channel (blue), followed by a merge of only the receptor signals within the cell.

(B) ON α RGCs co-labeling with gephyrin across development. Gephyrin signal within the cell (yellow) is overlaid on the RGC channel (blue). For (A) and (B), below the full RGC 3D view is a short dendritic segment at higher magnification (regions selected for each stack annotated with a rectangle).

(C) Quantification of the percentage dendritic occupancy of each postsynaptic marker (GABA_A α 3, green; gephyrin, yellow; GlyR α 1, magenta) within developing ON α RGCs. Number of cells quantified at each time point in parenthesis (the different colors correspond to the number of cells analyzed for the specific synaptic marker). $N = 3$ animals. P8 versus P12 GABA_A α 3 ($p = 0.0135$) and P8 versus P12 GlyR α 1 ($p = 0.0025$) RGC occupancies were significantly different. An unpaired two-tailed t test was performed. Scale bars, 30 μ m.

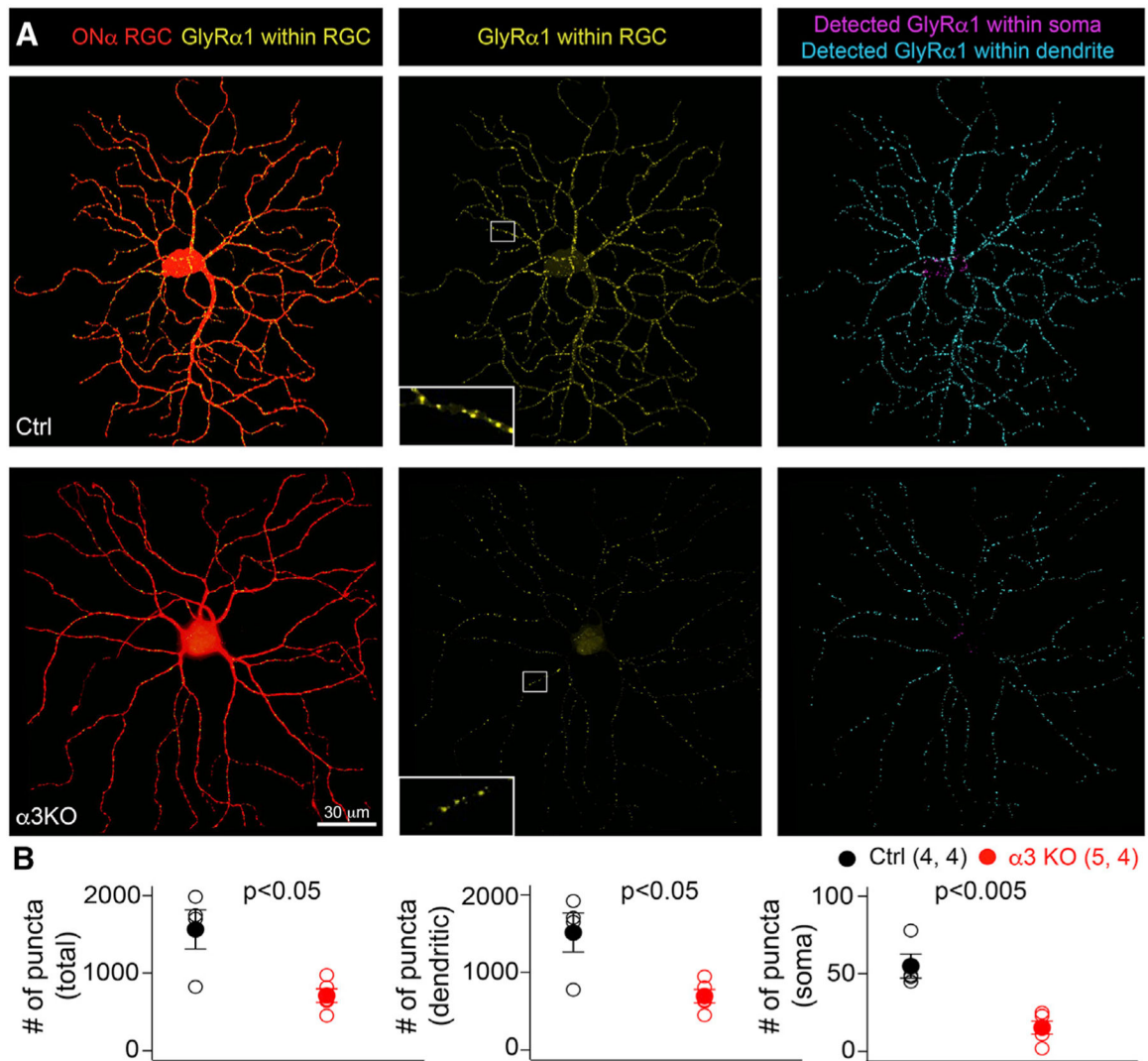


Figure 6. ON α GlyR clusters are downregulated in the GABA $_A$ α 3KO

(A) Three-dimensional (3D) en face view of an ON α RGC (red) in littermate control (Ctrl; top panel) and GABA $_A$ α 3KO (α 3KO; bottom panel) in *Thy1-YFP* \times GABA $_A$ α 3KO double-transgenic immunolabeled for glycine receptor α 1 sites (GlyRa1, yellow; insets show higher magnification view of select dendritic segments). Detected GlyRa1 within the soma (magenta) and dendritic arbor (cyan) of the ON α were both downregulated in the α 3KO RGC compared with Ctrl.

(B) Quantification of the total number of detected GlyRa1 puncta, GlyRa1 puncta within the dendrites, and GlyRa1 puncta within the ON α RGC soma in the α 3KO and Ctrl. All fractions of GlyRa1 are significantly reduced in the α 3KO compared with Ctrl. Numbers in parentheses are number of cells, number of animals sampled. An unpaired two-tailed t test was performed.

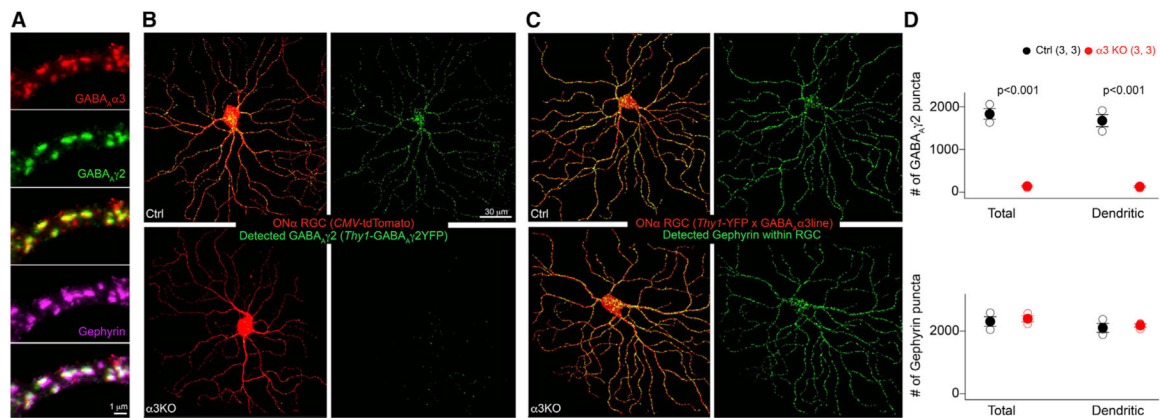


Figure 7. GABA_Aγ2 but not gephyrin is downregulated across ONα arbors in the absence of GABA_Aα3

(A) Dendritic segment of an ONα RGC in the *Thy1-GABA_Aγ2YFP* (green) transgenic line with co-labeling for GABA_Aα3 (red) and gephyrin (magenta) demonstrating that these postsynaptic proteins are colocalized across ONα inhibitory synapses.

(B) Three-dimensional (3D) en face view of ONα RGCs in littermate control (Ctrl; top panel) and GABA_Aα3KO (α3KO; bottom panel) retina crossed into the *Thy1-GABA_Aγ2YFP* line. ONα RGCs in the *Thy1-GABA_Aγ2YFP* × GABA_Aα3KO double-transgenic were visualized by biolistic transfection (*CMV-tdTomato*; red). GABA_Aγ2 receptor puncta detected within the ONα RGC (green) are downregulated in the α3KO.

(C) Co-labeling of ONα (red) in Ctrl (top panel) and α3KO-*Thy1-YFP* (bottom panel) retina with gephyrin (detected puncta within RGC visualized in green).

(D) Top panel: quantification of total and dendritic GABA_Aγ2 puncta within Ctrl and α3KO ONα RGCs. Bottom panel: quantification of total and dendritic gephyrin puncta within Ctrl and α3KO ONα RGCs. Numbers in parentheses are number of cells, number of animals sampled. An unpaired two-tailed t test was performed.

KEY RESOURCES TABLE

REAGENT or RESOURCE	SOURCE	IDENTIFIER
Antibodies		
Chicken anti-GFP	Abcam	Catalog # ab13970; RRID: AB_300798
Mouse monoclonal anti-GlyR α 1	Synaptic Systems	Catalog # 146111; RRID: AB_887723
Guinea pig polyclonal anti-GABA α 1	Fritschy and Mohler 1995	Generated in Jean-Marc Fritschy's Lab
Guinea pig polyclonal anti-GABA α 3	Fritschy and Mohler 1995	Generated in Jean-Marc Fritschy's Lab
Mouse monoclonal anti-gephyrin	Synaptic Systems	Catalog # 147111; RRID: AB_887719
Chemicals, peptides, and recombinant proteins		
Ames	Sigma	A1420
SR-95531 (GABAzine)	Sigma	S106
TTX	Abcam	120055
Strychnine	Sigma	S8753
Alexa 594	ThermoFisher	A10442
NBQX	Tocris	0373
D-AP5	Tocris	0106
Vectashield antifade mounting medium	Vector Labs	Catalog# H-1000
Experimental models: organisms/strains		
Mouse: <i>Thy1-YFPH</i>	R. Wong (Feng et al., 2000)	N/A
Mouse: GABA α 3 knockout	U. Rudolph (Yee et al., 2005)	N/A
Mouse: <i>Thy1-YFPγ2</i>	R. Wong (Bleckert et al., 2013)	N/A
Mouse: C57BL/6J	Jackson Labs	JAX Stock No: 000664
Recombinant DNA		
CMV-tdTomato	R. Wong, University of Washington (Morgan et al., 2008)	N/A
CMV-PSD95CFP	Construct modified from PSD95-YFP construct from A.M. Craig, University of British Columbia (Kerschensteiner et al., 2009)	N/A
Software and algorithms		
IGOR Pro	WaveMetrics	https://www.wavemetrics.com/
MATLAB	Mathworks	https://ch.mathworks.com/products/matlab.html
Symphony	Symphony-DAS	https://github.com/symphony-das
ImageJ	NIH	https://imagej.nih.gov/ij/
Amira	ThermoFisher Scientific	https://www.thermofisher.com/global/en/home/industrial/electron-microscopy/electron-microscopy-instruments-workflow-solutions/3d-visualization-analysis-software/amira-life-sciences-biomedical.html

REAGENT or RESOURCE	SOURCE	IDENTIFIER
KNOSSOS	Max Planck Institute for Medical Research, Heidelberg, Germany	https://knossos.app
Neuromatic	Rothman & Silver, 2018	http://www.neuromatic.thinkrandom.com/

Author Manuscript

Author Manuscript

Author Manuscript

Author Manuscript